ELSEVIER

Deep-Sea Research II 51 (2004) 2041–2072

DEEP-SEA RESEARCH
PART II

www.elsevier.com/locate/dsr2

Acoustically-inferred zooplankton distribution in relation to hydrography west of the Antarctic Peninsula

Gareth L. Lawson[a,b,*], Peter H. Wiebe[b], Carin J. Ashjian[b], Scott M. Gallager[b], Cabell S. Davis[b], Joseph D. Warren[c]

[a]*MIT/Woods Hole Oceanographic Institution Joint Program in Oceanography, Woods Hole, USA*
[b]*Biology Department, Woods Hole Oceanographic Institution, Woods Hole, MA 02543, USA*
[c]*Southampton College, 239 Montauk Hwy, Southampton, NY 11968, USA*

Accepted 12 July 2004

Abstract

The relationship between the distribution of zooplankton, especially euphausiids (*Euphausia* and *Thysanoessa* spp.), and hydrographic regimes of the Western Antarctic Peninsula continental shelf in and around Marguerite Bay was studied as part of the Southern Ocean GLOBEC program. Surveys were conducted from the RVIB *N.B. Palmer* in austral fall (April–June) and winter (July–August) of 2001. Acoustic, video, and environmental data were collected along 13 transect lines running across the shelf and perpendicular to the Western Antarctic Peninsula coastline, between 65°S and 70°S. Depth-stratified net tows conducted at selected locations provided ground-truthing for acoustic observations. In fall, acoustic volume backscattering strength at 120 kHz was greatest in the southern reaches of the survey area and inside Marguerite Bay, suggestive of high zooplankton and micronekton biomass in these regions. Vertically, highest backscattering was in the 150–450 m depth range, associated with modified Circumpolar Deep Water (CDW). The two deep troughs that intersect the shelf break were characterized by reduced backscattering, similar to levels observed off-shelf and indicative of lower zooplankton biomass in recent intrusions of CDW onto the continental shelf. Estimates of dynamic height suggested that geostrophic circulation likely caused both along- and across-shelf transport of zooplankton. By winter, scattering had decreased by an order of magnitude (10 dB) in the upper 300 m of the water column in most areas, and high backscattering levels were found primarily in a deep (>300 m) scattering layer present close to the bottom. The seasonal decrease is potentially explained by advection of zooplankton, vertical and horizontal movements, and mortality. Predictions of expected backscattering levels based on net samples suggested that large euphausiids were the dominant source of backscattering only at very particular locations and depths, and that copepods, siphonophores, and pteropods were more important in many locations.

*Corresponding author. Tel.: +1 508 289 3649; fax: +1 508 457 2134.
E-mail address: glawson@whoi.edu (G.L. Lawson).

0967-0645/$ - see front matter © 2004 Elsevier Ltd. All rights reserved.
doi:10.1016/j.dsr2.2004.07.022

1. Introduction

Zooplankton play a pivotal role in the antarctic continental shelf ecosystem, providing both a trophodynamic link between phytoplankton and higher predators, and, via their faecal pellets, a mechanism by which newly fixed carbon can be exported from the euphotic zone (Priddle et al., 1992). Historically, much attention has focused on Antarctic krill (*Euphausia superba*) due to its status as a key prey item for many whales, birds, seals, and fishes (Laws, 1985) and as the subject of a commercial fishery (Ichii, 2000). Although less studied, other zooplankton also represent important ecosystem members: copepods, for example, frequently exceed Antarctic krill in abundance and are the main prey of invertebrates, sei whales, and fish (Voronina, 1998), while salps may account for more carbon export to depth than Antarctic krill (Le Fèvre et al., 1998).

High-frequency acoustic sensors are often used in the study of zooplankton distribution, due to their high sampling rates and concomitant ability to survey the entire water column over large areas (Foote and Stanton, 2000). In the Antarctic, acoustic techniques are used routinely to survey the biomass and distribution of Antarctic krill (see review by Hewitt and Demer, 2000), but have been used much less frequently to study other zooplankton taxa (Weeks et al. 1995; Brierley et al., 1998). Substantial progress has been made in discriminating Antarctic krill from other acoustic scatterers that may be present (Madureira et al., 1993; Brierley et al., 1998; Watkins and Brierley, 2002; Hewitt et al., 2003). Historically, however, many Southern Ocean acoustic studies have simply assumed that all volume backscattering strength measurements above some minimum threshold stemmed from Antarctic krill (e.g., Macaulay et al., 1984; Lascara et al. 1999; Nicol et al., 2000). The contribution to acoustic observations from other zooplankton taxa often has been assumed to be negligible, which discards potential information on the biomass and distribution of such taxa, and may result in an overestimation of Antarctic krill abundance.

The continental shelf region in and around Marguerite Bay, west of the Antarctic Peninsula (Fig. 1), is hypothesized to be an important over-wintering ground for Antarctic krill, and may act as a source for the down-stream krill populations in the Bransfield Strait and at South Georgia (Atkinson et al., 2001; Fach et al., 2002). Little is known about the winter distribution of Antarctic krill or other zooplankton in this area, however, although studies of the nearby Bransfield Strait region have been more numerous (e.g., Siegel, 1989; Zhou et al., 1994). In the only previous acoustic survey of the region, Lascara et al. (1999) examined Antarctic krill distribution in Marguerite Bay and the region immediately to the north, and found distinct seasonal variability in biomass and vertical distribution, with krill more abundant and shallower during the summer and spring than fall and winter. The acoustic system employed reached to only 189 m in depth, and so this study was unable to conclude whether the seasonal decrease in biomass resulted from vertical or horizontal movements. Given the dearth of previous studies, the US Southern Ocean GLOBal ECosystems Dynamics (SO GLOBEC) program has targeted austral fall and winter as periods for detailed study of the Marguerite Bay region (Hofmann et al., 2002). The program's primary objective is to understand the physical and biological factors that contribute to Antarctic krill over-wintering success. As such, one goal of the program is to link physical processes with the distribution of Antarctic krill and other members of the zooplankton community, and ultimately with higher predators.

In this paper, we describe measurements of acoustic volume backscattering strength made over most or all of the water column during austral fall and winter of 2001, in relation to hydrography in the vicinity of Marguerite Bay. We then use depth-stratified net samples and taxon-specific models of acoustic target strength to predict the likely sources of acoustic backscattering, with particular emphasis on understanding the contribution of zooplankton taxa other than Antarctic krill. On the basis of these measurements and predictions, we make certain inferences concerning seasonal and spatial variability in zooplankton and micronekton biomass in the region.

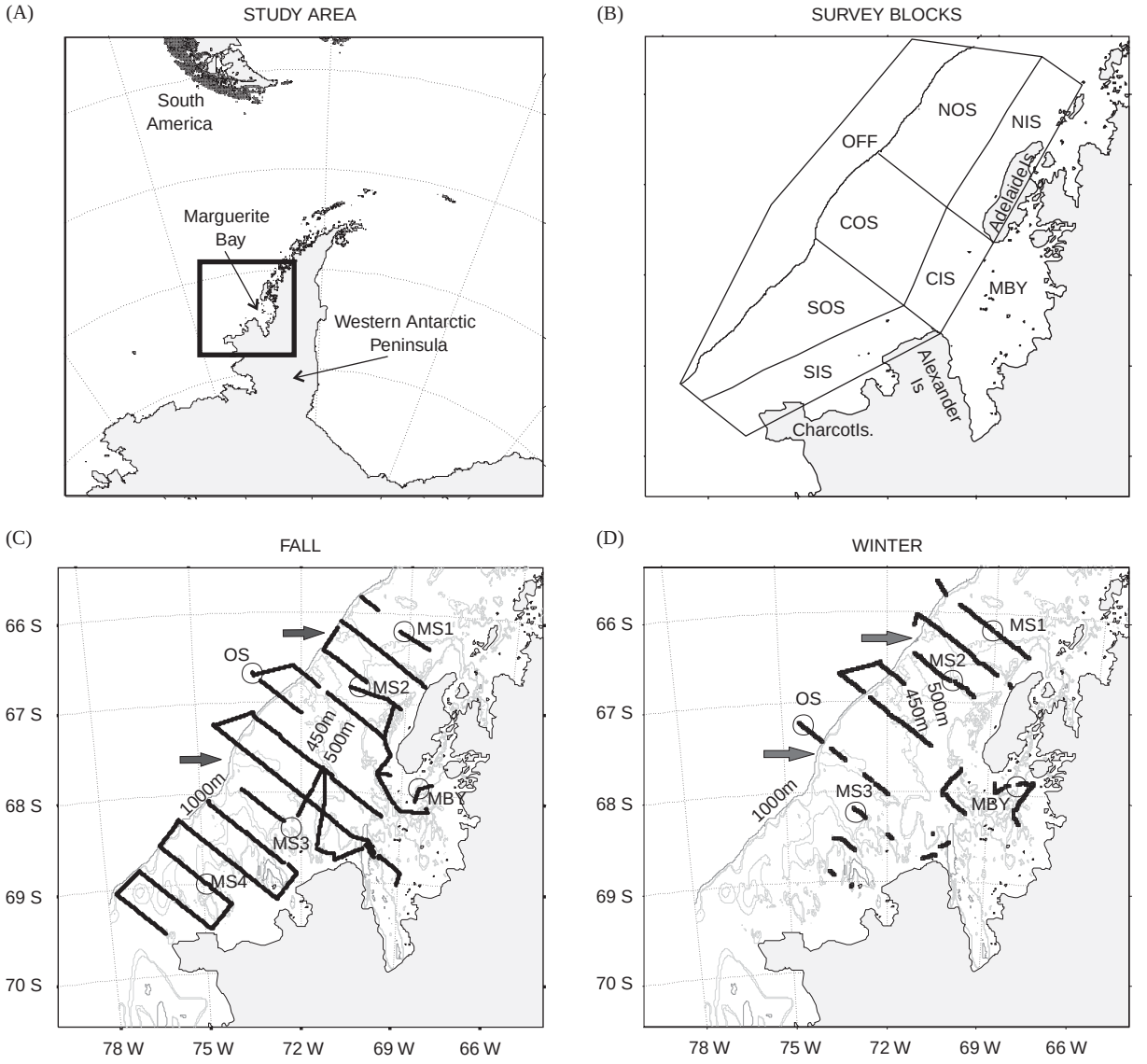

Fig. 1. US SO GLOBEC survey area. Shown are (A) the overall geographical context of the survey area, (B) the location of survey blocks, and the cruise tracks in (C) fall and (D) winter 2001. The latter show only those portions of the overall cruise-track where acoustic data were collected. Note the lower survey coverage in winter relative to fall. Block name abbreviations are: Northern Outer-Shelf (NOS), Northern Inner-Shelf (NIS), Central Outer-Shelf (COS), Central Inner-Shelf (CIS), Southern Outer-Shelf (SOS), Southern Inner-Shelf (SIS), Off-Shelf (OFF), and Marguerite Bay (MBY). Circles indicate where the MOCNESS tows analyzed here were conducted, with tow locations abbreviated as mid-shelf 1-4 (MS1-4), off-shelf (OS), and Marguerite Bay (MBY). Gray arrows show where the deep troughs that run diagonally across the continental shelf meet the shelf break.

2. Methods

2.1. Study area

The US SO GLOBEC Program study site was located on the continental shelf to the west of the Western Antarctic Peninsula, extending from the northern tip of Adelaide Island to the southern portion of Alexander Island and including Marguerite Bay (Fig. 1). Two cruises were conducted in the area on the RVIB *Nathaniel B. Palmer*: an austral fall cruise from April 23 to June 6, 2001 (cruise number NBP0103), and a winter cruise from July 21 to September 6, 2001 (cruise number NBP0104). The fall cruise track was determined by the position of 84 station locations distributed along 13 transect lines running across the continental shelf and perpendicular to the Peninsula coastline. On the winter cruise, eight additional stations were added to the survey grid and the entire grid was shifted south by 2 km so that acoustic mapping of the sea floor would take place over unmapped sea floor. In order to allow spatial comparisons across the region, the overall study area was subdivided into eight functional blocks (Fig. 1B). The survey region first was subdivided from northeast to southwest into three sectors (southern, central, and northern), each of which was divided into inner-shelf (i.e. coastal) and outer-shelf blocks. An off-shelf block was defined as the region beyond the 1000 m isobath, and a final block corresponded to the interior of Marguerite Bay.

2.2. BIOMAPER-II

The BIo-Optical Multi-frequency Acoustical and Physical Environmental Recorder, or BIOMAPER-II, is a towed system designed to conduct quantitative surveys of the spatial distribution of plankton and nekton (Wiebe et al., 2002). The system consists of a multi-frequency echosounder, a Video Plankton Recorder (VPR, Davis et al., 1992), and an environmental sensor package (Conductivity, Temperature, and Depth sensor (CTD); fluorometer; transmissometer). To enhance the performance of the BIOMAPER-II in high sea states, a slack tensioner was used to damp the motion of the ship (see Wiebe et al., 2002 for additional details).

2.2.1. Acoustic data collection

The BIOMAPER-II collected acoustic data from five pairs of transducers, with frequencies of 43, 120, 200, 420, and 1000 kHz. All transducers had 3° half-power beamwidths, with the exception of the 43 kHz transducers, which had beamwidths of 7°. One of each pair of transducers was mounted on the top of the tow-body looking upward, while the other was mounted on the bottom looking downward. This arrangement allowed acoustic data to be collected over most or all of the water column as the instrument was 'towyoed' obliquely up and down through the water column between 20 and 300 m depth. The vessel proceeded along the track-line between stations at 4–6 knots, and surveying was conducted around the clock.

Multi-frequency acoustic data were collected over much of both surveys, although prohibitively thick pack ice in portions of the survey area led to the area surveyed in winter being less than in fall (Figs. 1C and D). Due to episodic malfunctions at the different acoustic frequencies, 120 kHz represents the frequency at which data were collected with the greatest spatial coverage. In order to allow examinations of the seasonal distribution of zooplankton over the broadest scales possible and best complement the scales at which data were collected by other projects conducted during the cruises (e.g., top predator surveys), this paper deals only with acoustic data collected at 120 kHz. Analyses of the multi-frequency data will be the subject of future papers.

Volume backscattering strength, S_v (where $S_v = 10 \log_{10} s_v$ in units of decibels, and s_v is the observed volume backscattering coefficient), is a measure of the intensity of emitted sound that is reflected back to the source per cubic meter. For simplicity, this quantity will be referred to as 'backscattering.' Backscattering is related to both the number and size of scatterers in the path of the incident sound, to the efficiency with which these scatterers reflect sound, and thereby to their taxonomic composition. Although the relationship

between backscattering and the biomass of scatterers is thus highly complex, we assume that the large spatial and temporal differences in backscattering observed in the present study are related to differences in zooplankton and micronekton biomass. In the discussion we show how the confounding influences of animal size, sound scattering efficiency, and taxonomic composition, are minimized in this study.

Backscattering data at 120 kHz were collected in 1.5-m-deep bins, starting at 6 m from the transducer face (the end of the acoustic near-field) and extending to a maximum range of 300 m from the instrument. A 10 kHz bandwidth chirp pulse was used (Ehrenberg and Torkelson, 2000), with an effective pulse duration of 0.18 ms, and a ping rate of 0.3 pings s^{-1}. The system's dynamic range allowed these data to be collected between −100 and −40 dB. Profiles of noise levels (ship's noise, ambient noise, and system noise combined) vs. depth were made in situ near the start of each cruise. Backscattering levels in each ping were compared to these profiles, and those bins where backscattering did not exceed noise levels were set to zero. Backscattering data were echo-integrated over 4-ping intervals (i.e., ~35 m along-track).

All transducers were acoustically calibrated by the manufacturer (Hydroacoustic Technologies Inc., Seattle, WA, USA) prior to each cruise for source level, receive sensitivity, as well as transmit and receive beam patterns. An in situ calibration also was performed at the end of the winter cruise with a 38 mm tungsten carbide (6% cobalt) standard target, following established practices (Foote et al., 1987). This calibration indicated that the standard target was approximately 6 dB lower on the down-looking 120 kHz transducer than it should have been, and the data therefore were corrected for this offset. Although there is no reason to doubt the validity of the calibration, 6 dB is a large correction and it must be noted that the absolute levels of backscattering reported here thus may contain some bias. The relative changes in backscattering that are the focus of this paper and our conclusions would not be affected by any such bias. After backscattering data were corrected for the results of these calibrations, there was evidence of higher backscattering levels observed by the up-looking 120-kHz transducer relative to the down-looking transducer in some portions of the water column (Fig. 2). This discrepancy was particularly evident in low-scattering areas such as the northern portion of the survey area in fall, and much of the continental shelf during winter; in high-scattering areas like Marguerite Bay, no such difference was evident. Furthermore, the enhanced backscattering levels in the up-looking data were restricted to the pycnocline and were especially prominent in regions of rapid vertical changes in density. We believe that these enhancements do not represent scattering from biological sources, but rather represent an as-yet unexplained artifact. They may result from sound reflecting off vortices shed by the tow cable as it passes through the pycnocline. Since the tow cable extends above the towed body, only the up-looking transducer would observe such artifactual backscattering. It therefore was excluded from all quantitative analyses, representing a 7% reduction in data (varying from 0% to 24% on a by-transect basis), primarily between 0 and 200 m.

2.2.2. *Acoustic data post-processing*

Acoustic data from the up- and down-looking transducers were combined to provide a vertically continuous acoustic record extending from the surface to at least 300 m, and at most 550 m, depending on the position of the BIOMAPER-II along its towyo path. This acoustic record then was edited using custom MATLAB-based routines to remove unwanted returns from the surface bubble layer and the bottom, as well as noise spikes from the ship's engines or ice-breaking.

For many of the following spatial analyses, measurements of integrated backscattering in each 1.5-m depth bin were averaged over 1-km along-track intervals and also over depth, in intervals of 25–100 m (shallow layer), 100–300 m (mid-water layer), and 300–500 m (deep layer). These depth ranges were chosen since the surface bubble layer obscured most measurements shallower than 25 m, the mixed-layer depth was generally around 100 and 300 m represents the depth to which the BIOMAPER-II always made acoustic observations despite being towyoed up and down through

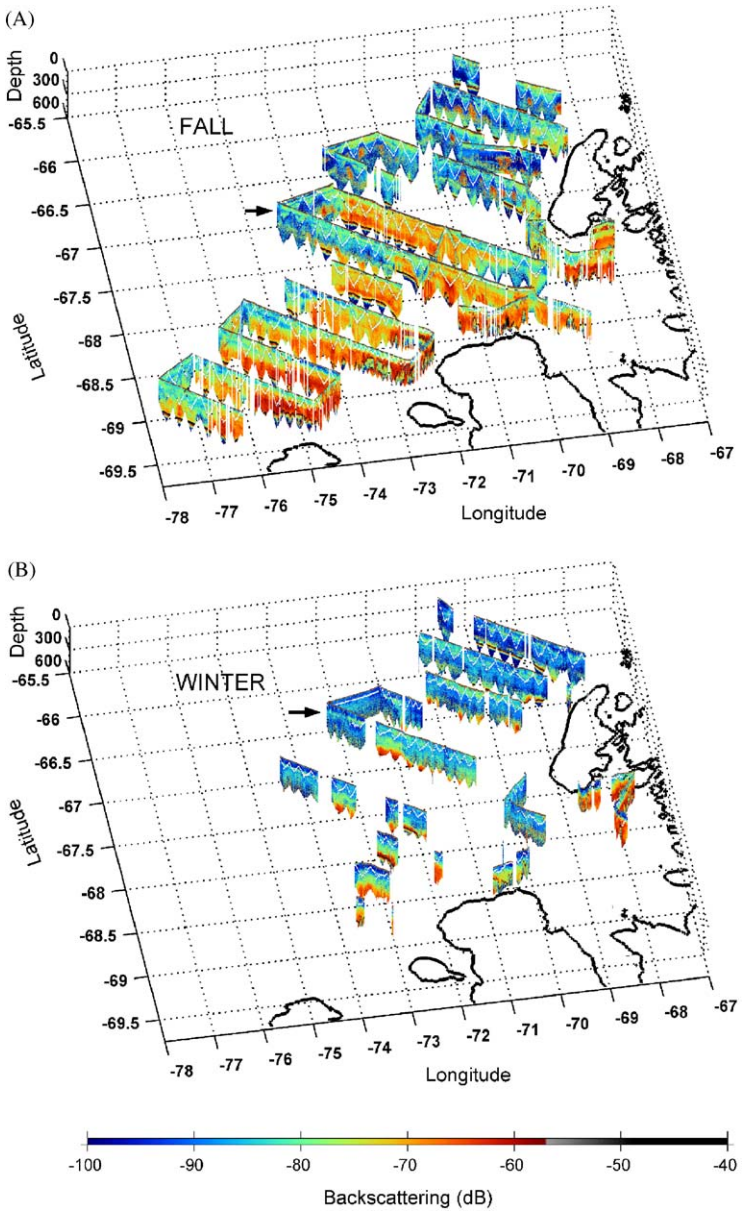

Fig. 2. Acoustic data collected in (A) fall and (B) winter 2001. Backscattering levels are plotted on the color scale in decibels, according to the depth and position of measurement. Blue indicates low levels of zooplankton backscattering, while red to black indicate high levels. High backscattering near the surface corresponds to the surface bubble layer. Strong (i.e. black) returns at depth are from the strongly reflecting bottom. Both the bottom and surface layer were edited out for quantitative analyses. The V-shape of the maximum depth of observation is due to the BIOMAPER-II being towyoed up and down through the water column as the vessel proceeded along-track. Arrows indicate typical regions of the pycnocline where enhanced backscattering measured by the up-looking transducer (i.e. in the upper portion of the towyo's V) was believed to represent an artifact rather than scattering from biological sources.

the water column. These averages, as well as all other simple descriptive statistics, were calculated using the arithmetic form of backscattering (s_v). The arithmetic form also was used in between-block statistical comparisons, since the tests employed were rank-based (see below) and so insensitive to whether the data were transformed or not. The decibel form of backscattering (S_v) was used in regression analyses, since this test is parametric and the log-transformed data better approximated a normal distribution. The decibel form is also used in figures and in the text.

2.3. Environmental analyses

Acoustic data were combined with environmental data to examine the association of backscattering with environmental properties and water masses. Depth, temperature, conductivity, fluorescence, and transmissometry data were collected by the BIOMAPER-II along its towyo path at 4-s intervals. In order to provide details of the environmental structure at greater depths than sampled by the towed body, however, data from CTD casts made at the survey stations by Klinck et al. (2004) were used as the primary source for quantitative analyses. The CTD rosette package made measurements of salinity, fluorescence, transmittance, photosynthetically active radiation (PAR), potential temperature, and oxygen concentration at 1-m depth intervals from the surface to between 5 and 20 m off the bottom. In analyses of backscattering in relation to environmental conditions, each environmental measurement was associated with the acoustic measurement averaged in 1-km intervals made nearest to that depth and location.

2.4. MOCNESS

A 1-m^2 Multiple Opening/Closing Net and Environmental Sensing System (MOCNESS; Wiebe et al., 1985) was used to sample the zooplankton at selected stations distributed throughout the survey grid (24 locations in fall and 17 in winter). The MOCNESS was equipped with nine 335-μm mesh nets, a suite of environmental sensors including temperature, conductivity, fluorescence, and light transmission, and a strong strobe light, that flashed at 4-s intervals. The rationale behind the strobe system was to shock or blind the animals temporarily so that the net would not be perceived and avoided, and catches of large euphausiids were significantly enhanced when using the strobe (Sameoto et al., 1993; Wiebe et al., 2004). The MOCNESS was towed obliquely from near-bottom to the surface, sampling eight depth intervals on the up-cast. The deepest tows sampled to 1000 m. Typically, the upper 100 m were sampled in 25-m intervals, with 50-m intervals at intermediate depth ranges, and greater intervals (150- or 200-m) for the deepest depth ranges (see Ashjian et al., 2004, for additional details). The depth-specific samples were preserved upon recovery in 4% buffered formalin.

The size distributions of plankton for six MOCNESS tows from each of the two cruises have been analyzed to date (Ashjian et al., 2004). Following the nomenclature of Ashjian et al. (2004), tow locations will be referred to as off-shelf, Marguerite Bay, and mid-shelf 1–4 (Figs. 1C,D). Note that no acoustic data were collected in the vicinity of the winter mid-shelf 4 site. Lengths of individuals of each sampled taxon were determined for an aliquot of each net sample using the silhouette method of Davis and Wiebe (1985).

2.5. Taxonomic composition of zooplankton and micronekton

The ultimate goal of our research is to use VPR observations and taxon-specific differences in backscattering at increasing frequencies, in addition to net catches, to partition accurately our measurements of backscattering among taxonomic groups, and then to make biomass estimates for each taxon. Here, we make preliminary inferences concerning the sources of acoustic backscattering measurements by conducting the forward problem: an exercise where predictions are made of expected levels of backscattering based on MOCNESS catches and models of the backscattering from individual sampled animals (Wiebe et al., 1996). By comparing these predictions to observed

backscattering levels, it is possible to assess whether the animals collected by the nets could account for measured levels of backscattering. Provided that this assessment is favorable, inferences can then be made about the likely relative contributions of different taxa to observed backscattering levels in the vicinity of each tow.

In addressing the forward problem, predicted backscattering levels for each depth stratum sampled by the MOCNESS were calculated as the linear (i.e. incoherent) sum of expected echo intensities from each captured animal. Expected echo intensities, or backscattering cross-sections $\langle \sigma_{bs} \rangle$ were estimated based on the length of each individual determined by silhouette analysis and models of acoustic scattering appropriate to the individual's taxonomic group. These models were developed by Stanton et al. (1994, 1998), are reviewed in Stanton and Chu (2000), and are sensitive to numerous parameters in addition to animal length, including animal orientation and material properties (Chu et al., 2000; Table 1). Discrete values were used for all parameters other than animal orientation (Table 1). For the latter, scattering from each animal was averaged over some distribution of orientations, to allow for the fact that the animals are oriented at a range of angles as they move through the water.

Estimates of expected backscattering cross-sections for each *j*th individual were summed over all individuals in each *i*th taxon and then over all taxa to yield an estimate of the total expected volume backscattering strength (S_v, in dB) in the volume (V) defined by the depth range sampled by each *k*th net:

$$S_{v_k} = 10 \log_{10} \left[\frac{1}{V_k} \sum \sum \langle \sigma_{bs} \rangle_{ij} \right].$$

Since the BIOMAPER-II and the MOCNESS could not be towed concurrently, comparisons of predicted backscattering levels could not be made to observations of backscattering made at the identical time and location. Comparisons were thus made to acoustic observations made in the appropriate depth interval and averaged over a spatial area within no more than 17 km of each of the 11 MOCNESS tows. At all but two MOCNESS tow locations, acoustic data were collected within no more than 5 h of the net tow as the vessel approached or departed the station. At the mid-shelf 1 and 2 stations in winter, however, MOCNESS tows and acoustic data collection were separated in time by approximately four weeks due to instrument problems. Predictions of backscattering from each taxon were still calculated based on these tows, in order to shed light on the sensitivity of the predicted to observed backscattering comparison to temporal variation.

3. Results

Backscattering during fall generally was enhanced within Marguerite Bay and in the southern portion of the survey area (Fig. 2A). Large subsurface patches of intensified backscattering that stood out markedly from background scattering levels were observed primarily in coastal regions of complex bathymetry, and at depth in the northern portion of the continental shelf. The term 'patch' is used here to denote a recognizable feature in the acoustic record, but does not imply any particular aggregative behavior on the part of the zooplankton or micronekton comprising these features. Smaller such patches also were evident within the mixed layer across the shelf. In winter, the most striking feature was a dramatic decrease in backscattering relative to fall levels throughout most of the water column (Fig. 2B); backscattering in winter was high only within Marguerite Bay and in the bottom scattering layer, which was present on both cruises.

3.1. Environmental setting

The continental shelf in this region is characterized by intrusions of oceanic Circumpolar Deep Water (CDW; salinity (S) 34.6–34.74, potential temperature (θ) 1.0–2.0 °C), pumped up onto the shelf at depth by the action of the Antarctic Circumpolar Current (see Klinck et al., 2004; and Smith et al., 1999, for further water mass definitions and descriptions of hydrography). As this warm and salty CDW interacts with cooler and fresher shelf waters, it forms a water mass that has been referred to as modified-Circumpolar Deep

Water (mCDW, *sensu* Hofmann and Klinck, 1998; S 34.0–34.6, θ −1.8 to 1.5 °C). Such mCDW was the primary water mass observed through the pycnocline and below in the study area, often with CDW present at greater depths (Table 2). During fall, the water column at shallow depths contained Antarctic Surface Water (AASW, Table 2; S 33.0–33.7, θ −1.5 to 1.0 °C). In winter, AASW was mostly replaced near the surface in all survey blocks by Winter Water (WW; S 33.8–34.1, θ −1.8 to −1.5 °C). Water properties differed between regions. The mCDW found during fall in the more northern and more offshore blocks was generally warmer and saltier (i.e. less-modified) than elsewhere in the study area, suggesting more recent intrusions of CDW onto the shelf. The more coastal regions typically had warmer and fresher AASW present at shallow depths, particularly in Marguerite Bay.

3.2. Vertical distribution of backscattering

Seasonal and spatial differences were observed in the vertical distribution of backscattering (Fig. 3). In fall, backscattering was strongest between 150 and 450 m in all of the inner-shelf and southern blocks. Scattering in the northern and central outer-shelf blocks was more constant with depth. A slight enhancement in backscattering was observed in all blocks at shallower depths (15–95 m, depending on block), corresponding to the influence of episodic patches of high backscattering present within the mixed layer. The decrease in backscattering from fall to winter was also evident in the vertical distribution of backscattering. Backscattering throughout the upper 300 m of the water column in winter was very low in all blocks except Marguerite Bay and the two southern blocks. Below 300 m, however, backscattering generally increased rapidly, and in all but one block reached levels higher than those observed at comparable depths during fall. This increase at depth was due to the influence of the deep scattering layer associated with the bottom, which was present during both surveys, but more intense in winter (Fig. 2).

3.3. Horizontal distribution of backscattering

The horizontal distribution of backscattering was examined via comparisons between geographically defined spatial blocks and spatial interpolations of backscattering data between transect lines using linear kriging (Chu, 2000; Fig. 4). During fall, backscattering in the mid-water (100–300 m) and bottom (300–500 m) depth ranges spatially averaged over 1-km intervals differed significantly between survey blocks (Kruskal-Wallis non-parametric one-way analysis of variance (Sokal and Rohlf, 2000), $\chi^2 = 809$, $p < 0.001$, $n = 1932$, and $\chi^2 = 573$, $p < 0.001$, $n = 1030$, respectively; Table 2), with highest levels in the southern inner-shelf and Marguerite Bay and lowest off-shelf (Tukey-Kramer post-hoc tests (Sokal and Rohlf, 2000), $p < 0.05$). Within the shallow layer (25–100 m), backscattering was reduced relative to the deeper layers, but showed similar enhancements in coastal areas, as well as significant differences between blocks ($\chi^2 = 367$, $p < 0.001$, $n = 1385$).

Marguerite Trough is the deep trough that cuts diagonally across the continental shelf, meeting the shelf break at approximately 66.5°S (Figs. 1C,D and 4A,C); interpolations show that backscattering at depth was very low in the vicinity of this meeting point. A second trough meets the shelf break at approximately 67.75°S (Fig. 1C,D). Backscattering near this point was very low in the 100–300 m depth range, and reduced relative to nearby levels in the 300–500 m range. Hydrographic observations suggest that CDW intrudes on to the shelf at these locations (Figure 9 in Klinck et al., 2004; Dinniman and Klinck, 2004); the low observed backscattering levels are suggestive of low zooplankton biomass in these recently intruded waters. Contours of dynamic height relative to 400 m calculated by Klinck et al. (2004) indicate a cyclonic gyre situated in the northern portion of the survey area, and a coastal current moving along the shelf towards the southwest (Fig. 4E). Enhanced backscattering was evident in all three depth ranges at the southern end of this gyre, where water was flowing in an offshelf direction. Scattering also was enhanced in the vicinity of the coastal current off Alexander Island.

Table 1
Scattering models employed in forward calculations of backscattering levels expected based on MOCNESS catches

Taxon	Scattering model	Parameter values		
	(Ref. in parentheses)	Orientation (Ref.)	Density contrast (g) (Ref.)	Sound speed contrast (h) (Ref.)
Copepods*	Distorted-Wave Born Approximation (DWBA)-Based Fluid-Like Deformed Cylinder (1)	N(0,30)	1.02 (7)	1.058 (14)
Large Euphausiids* and Mysids (>15 mm)	DWBA Deformed Cylinder (1)	N(20,20) (6)	$g = 5.485 \times 10^{-4} \times \mathrm{L(mm)} + 1.002$ (8)	$h = 5.942 \times 10^{-4} \times \mathrm{L(mm)} + 1.004$ (8)
Small Euphausiids and Mysids (<15 mm)	DWBA Deformed Cylinder (1)	N(20,20) (6)	1.016 (8)	1.019 (8)
Amphipods	DWBA Deformed Cylinder (1)	N(0,30)	1.058 (9)	1.058 (9)
Chaetognaths and Polychaetes	DWBA Deformed Cylinder (1)	N(0,30)	1.03 (7)	1.03 (7)
Ostracods	DWBA Deformed Cylinder (1)	N(0,30)	1.03 (7)	1.03 (7)
Fish	DWBA Deformed Cylinder (1)	N(0,30)	1.03 (7)	1.03 (7)
Salps*	DWBA Deformed Cylinder (1)	N(0,30)	1.004 (10)	1.004 (10)
Gymnosome Pteropods	DWBA Deformed Cylinder (1)	N(0,30)	1.03 (7)	1.03 (7)
Larval Crustaceans	DWBA Deformed Cylinder (1)	N(0,30)	1.058 (9)	1.058 (9)
Eggs	High-Pass Fluid Sphere (2)	—	0.979 (11)	1.017 (11)
Thecosome Pteropods (*Limacina* spp.)*	High-Pass Fluid Sphere (2)	—	1.732 (10)	1.732 (10)
Radiolarians	High-Pass Fluid Sphere (2)	—	2.147 (12)	3.979 (12)
Medusae*	DWBA-based Model of Two Spheroidal Interfaces (3)	Broad-side only	1.02 (3)	1.02 (3)
Siphonophore Bracts and Nectophores	Scattering proportional to the volume of a fluid-filled sphere of equivalent volume (4)	—	1.02 (7)	1.02 (7)
Siphonophore Pneumatophores*	Carbon Monoxide-filled Sphere (5)	—	$g = g_{\mathrm{surface}}(1 + 0.1\mathrm{Depth(m)})$, where $g_{\mathrm{surface}} = 0.0012$ (13)	0.22 (15)

Asterisks (*) indicate those models that have been validated through comparisons of model predictions to laboratory measurements of scattering from the animal of interest; elsewhere, models were deemed appropriate on the basis of what is known about the animal's physical structure, but not on experimental verifications. Each model involves a number of parameters, describing the animal's shape, orientation, and acoustic material properties. The latter include the ratio of the animal's density to that of the surrounding water (g) and the ratio of the speed of sound in the animal to that in the surrounding water (h). Parameter values were drawn from a number of sources. All necessary shape parameters (e.g., length:width and length:volume ratios) were measured empirically for a sub-sample of captured animals. An average backscattering cross-section was calculated for each animal, based on a distribution of orientations. Where there was little or no information available on orientation, a normal distribution with a mean of 0° and a standard deviation of 30° was assumed (i.e. N(0,30)), where an angle of 0° indicates sound striking the animal in dorsal aspect. The taxa listed constituted the majority of sampled animals. Certain rare taxa (<3% of net abundance) were excluded from forward calculations; these included

thecosome *Styliola*-like pteropods, foraminifera, larval polychaetes, and ctenophores. Sensitivity analyses using scattering models for taxa comparable to these rare animals suggested that they were very minor contributors to overall backscattering levels (not shown).

(1) Equation (5) of Stanton et al. (1998), and see Stanton and Chu (2000) and references therein.

(2) Equation given in Stanton et al. (1994), p. 507.

(3) D. Chu. Unpublished Data.

(4) D. Chu. and A. Lavery, Pers. Comm.; Fluid-filled sphere model is derived from Anderson (1950).

(5) Derived from Anderson (1950).

(6) Chu et al. (1993).

(7) D. Chu. Pers. Comm.

(8) D. Chu. Unpublished Measurements; preliminary descriptions of results are found in US SO GLOBEC (2002). Measurements were performed only on animals larger than 20 mm.For animals smaller than this length (e.g., the 'small euphausiid' category), the g and h predicted by the regression equations for a 20 mm animal were assumed to apply.

(9) Inferred for shrimp based on model-fits to direct observations by Stanton et al. (1994), and very comparable to values measured by Chu et al. (2000) for the decapod shrimp *Palaemonetes vulgaris*. Assumed here to also apply to certain other crustacean taxa.

(10) Inferred based on model-fits to empirical observations, Stanton et al. (1994).

(11) Measured by Chu et al. (2003).

(12) Based on the density and sound speed of fused silica ($2.2\,g\,m^{-3}$ and $5968\,m\,s^{-1}$, respectively), and assuming the speed of sound in seawater is $1500\,m\,s^{-1}$, and the density of seawater is $1.025\,g\,m^{-3}$.

(13) A. Lavery. Pers. Comm.; based on pressure-related increases in density and thereby g in depth (Medwin and Clay, 1998). $g_{surface}$ is the density contrast for carbon monoxide at the surface (1 atmospheric pressure).

(14) Measured by Chu et al. (2000) for Gulf of Maine calanoid copepods.

(15) Sound speed contrast for carbon monoxide at surface pressure of 1 atmosphere.

Table 2
Between-block comparisons of environmental properties and backscattering

Block	Pot. temperature (Std Deviation)			Salinity			Mean (dB), Median (dB), and CV of backscattering			Day vs. night mean backscattering (dB)		
	25–100 m	100–300 m	300–500 m	25–100 m	100–300 m	300–500 m	25–100 m	100–300 m	300–500 m	25–100 m	100–300 m	300–500 m
Fall												
Northern Outer-Shelf	−0.84 (0.43)	1.02 (0.65)	1.44 (0.11)	33.95 (0.21)	34.57 (0.13)	34.71 (0.01)	Mean = −76.2 Med = −80.1 CV = 3.09	Mean = −70.9 Med = −76.1 CV = 1.33	Mean = −75.8 Med = −78.2 CV = 1.29	D = −74.4 N = −79.2	D = −70.5 N = −70.7	D = −74.3 N = −77.9
Northern Inner-Shelf	−0.33 (0.50)	0.70 (0.62)	1.37 (0.05)	33.74 (0.25)	34.45 (0.23)	34.69 (0.02)	Mean = −78.6 Med = −79.7 CV = 0.76	Mean = −68.6 Med = −72.8 CV = 1.49	Mean = −71.0 Med = −73.6 CV = 1.53	D = −79.4 N = −78.0	D = −69.1 N = −68.5	D = −72.6 N = −70.8
Central Outer-Shelf	−1.02 (0.26)	0.68 (0.81)	1.47 (0.08)	33.92 (0.19)	34.51 (0.16)	34.70 (0.01)	Mean = −72.2 Med = −73.2 CV = 0.88	Mean = −69.7 Med = −70.1 CV = 0.78	Mean = −67.8 Med = −68.4 CV = 0.72	D = −72.4* N = −71.8	D = −70.1* N = −69.4	D = −69.5* N = −67.2
Central Inner-Shelf	−0.44 (0.44)	0.49 (0.55)	1.27 (0.13)	33.74 (0.23)	34.38 (0.23)	34.67 (0.04)	Mean = −74.7 Med = −77.5 CV = 0.86	Mean = −64.6 Med = −71.2 CV = 4.52	Mean = −68.3 Med = −72.8 CV = 2.71	D = −72.0* N = −76.4	D = −59.2* N = −70.8	D = −65.1* N = −71.0
Southern Outer-Shelf	−1.24 (0.30)	0.09 (0.95)	1.31 (0.17)	33.75 (0.22)	34.40 (0.19)	34.68 (0.03)	Mean = −75.2 Med = −76.7 CV = 0.85	Mean = −69.6 Med = −70.6 CV = 0.90	Mean = −67.8 Med = −69.1 CV = 0.88	D = −76.8* N = −74.7	D = −70.4 N = −69.2	D = −68.4 N = −67.5
Southern Inner-Shelf	−0.99 (0.29)	−0.20 (0.64)	0.91 (0.16)	33.52 (0.23)	34.23 (0.23)	34.58 (0.05)	Mean = −71.0 Med = −74.0 CV = 2.42	Mean = −59.9 Med = −63.5 CV = 2.03	Mean = −64.2 Med = −64.1 CV = 0.46	D = −73.0 N = −70.3	D = −56.4 N = −62.9	D = −64.4 N = −64.1
Marguerite Bay	−0.42 (0.27)	0.38 (0.44)	1.07 (0.13)	33.48 (0.09)	34.28 (0.29)	34.61 (0.04)	Mean = −71.4 Med = −75.1 CV = 1.88	Mean = −67.4 Med = −67.6 CV = 0.49	Mean = −65.4 Med = −65.5 CV = 1.31	D = −77.4 N = −71.2	D = −71.4 N = −67.4	D = N.D. N = −65.3
Off-shelf	−1.05 (0.53)	1.11 (1.03)	1.78 (0.20)	33.92 (0.19)	34.51 (0.15)	34.69 (0.02)	Mean = −78.9 Med = −79.2 CV = 0.61	Mean = −73.2 Med = −77.0 CV = 1.25	Mean = −74.9 Med = −77.6 CV = 0.46	D = −77.7* N = −79.8	D = −77.2 N = −72.3	D = −73.7 N = −76.0

Winter

Northern Outer-Shelf	−1.70 (0.30)	0.90 (0.79)	1.49 (0.14)	33.96 (0.07)	34.22 (0.16)	34.71 (0.02)	Mean = −79.9 Med = −83.5 CV = 2.74	Mean = −82.7 Med = −83.4 CV = 0.66	Mean = −73.9 Med = −77.3 CV = 1.39	D = −82.9* N = −78.8	D = −83.6* N = −82.3	D = −74.0 N = −73.7
Northern Inner-Shelf	−1.08 (0.84)	0.77 (0.58)	1.45 (0.04)	33.98 (0.17)	34.49 (0.16)	34.69 (0.01)	Mean = −84.2 Med = −86.9 CV = 1.10	Mean = −81.5 Med = −85.5 CV = 1.64	Mean = −74.2 Med = −74.7 CV = 0.72	D = −84.3 N = −83.9	D = −86.2 N = −79.9	D = −74.9 N = −72.1
Central Outer-Shelf	−1.51 (0.40)	0.78 (0.65)	1.36 (0.06)	33.92 (0.12)	34.53 (0.16)	34.70 (0.05)	Mean = −83.4 Med = −84.5 CV = 1.07	Mean = −78.6 Med = −79.4 CV = 0.68	Mean = −65.7 Med = −65.9 CV = 0.45	D = −87.2* N = −83.0	D = −79.1 N = −78.0	D = N.D. N = −65.5
Central Inner-Shelf	−1.50 (0.39)	0.80 (0.66)	1.38 (0.04)	33.90 (0.11)	34.52 (0.17)	34.70 (0.01)	Mean = −78.4 Med = −84.8 CV = 4.66	Mean = −77.6 Med = −80.8 CV = 1.92	Mean = −74.6 Med = −77.6 CV = 0.94	D = −83.5* N = −75.5	D = −74.1 N = 79.2	D = −71.1 N = −76.9
Southern Outer-Shelf	−1.68 (0.22)	0.31 (0.68)	1.24 (0.08)	33.79 (0.07)	34.40 (0.20)	34.67 (0.02)	Mean = −88.4 Med = −91.5 CV = 1.18	Mean = −73.0 Med = −75.7 CV = 1.00	Mean = −61.8 Med = −61.2 CV = 0.47	D = −91.2 N = −85.6	D = −76.1 N = −69.1	D = −62.3 N = N.D.
Southern Inner-Shelf	−1.62 (0.22)	—	—	33.78 (0.05)	—	—	Mean = −81.6 Med = −80.6 CV = 0.72	Mean = −71.0 Med = −71.1 CV = 0.42	Mean = −67.2 Med = −67.8 CV = 0.80	D = N.D. N = −81.6	D = N.D. N = −71.0	D = N.D. N = −67.2
Marguerite Bay	−1.54 (0.35)	0.53 (0.58)	1.16 (0.04)	33.70 (0.12)	34.39 (0.24)	34.64 (0.01)	Mean = −78.6 Med = −82.5 CV = 1.18	Mean = −64.5 Med = −64.5 CV = 0.57	Mean = −61.3 Med = −61.7 CV = 0.59	D = −85.7* N = −76.9	D = −64.5 N = −64.2	D = −62.3 N = −60.5
Off-shelf	−1.56 (0.76)	0.77 (1.15)	1.71 (0.22)	33.97 (0.12)	34.47 (0.20)	34.69 (0.04)	Mean = −83.7 Med = −85.2 CV = 1.95	Mean = −82.6 Med = −82.6 CV = 0.45	Mean = −78.7 Med = −79.5 CV = 0.53	D = −85.2* N = −82.1	D = −83.5* N = −81.8	D = −78.5 N = −80.8

Mean potential temperature and salinity are shown, with standard deviations in parentheses. Mean, median, and coefficient of variation (CV) of backscattering were all calculated from backscattering measurements (arithmetic form, s_v) averaged over 1-km spatial intervals, and then over the three depth layers. Comparisons were made of mean day (D) and night (N) backscattering levels. In some cases, no data (N.D.) were collected during one or the other of the day/night periods in a given block. Asterisks (*) indicate instances where day backscattering within a given depth layer and block differed significantly ($p<0.05$) from night levels (Mann-Whitney non-parametric *t*-test equivalent, with significance levels Bonferroni-corrected for multiple tests). Note that the proportion of total survey time conducted during the day or night varied between blocks and seasons.

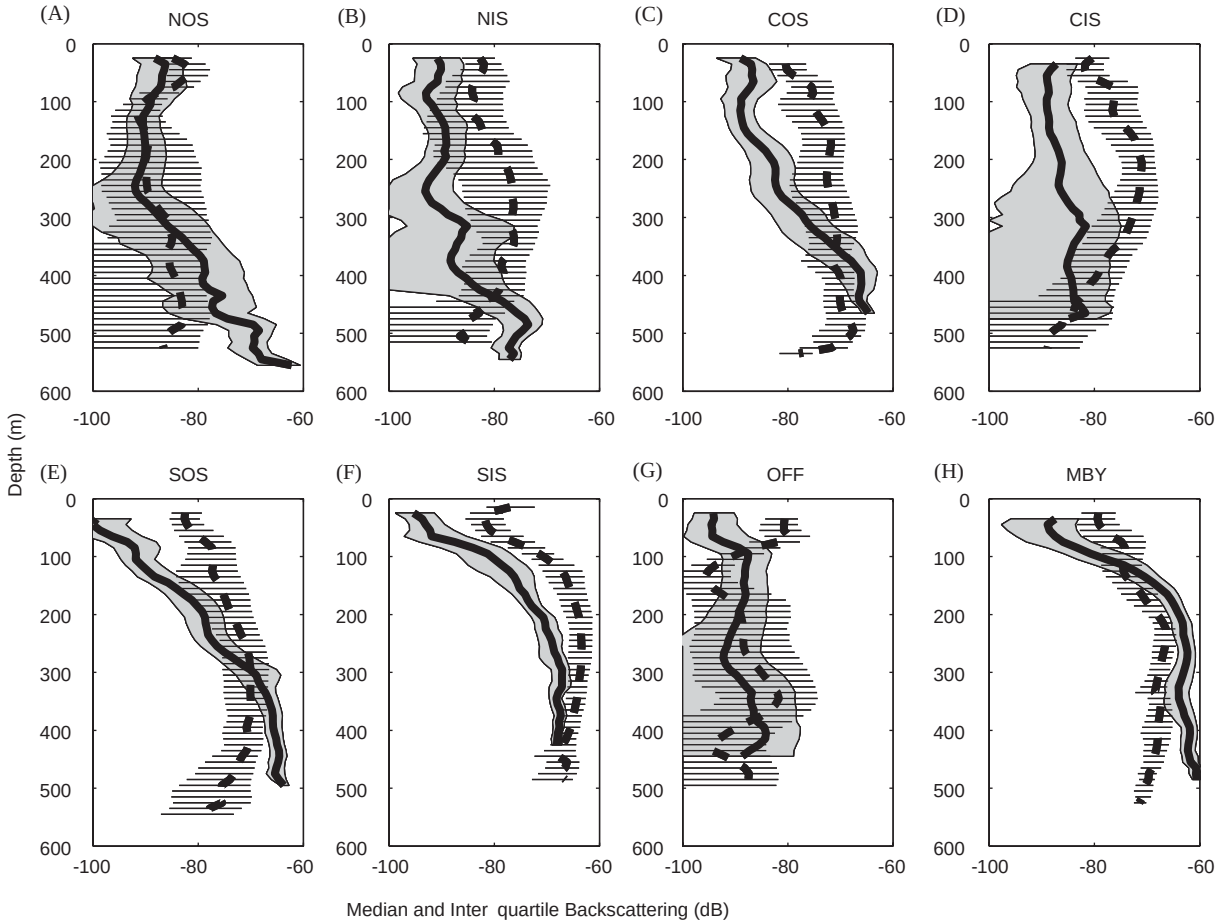

Fig. 3. Vertical distribution of backscattering in each survey block, during fall (dashed line) and winter (solid line), in the (A) Northern Outer-Shelf, (B) Northern Inner-Shelf, (C) Central Outer-Shelf, (D) Central Inner-Shelf, (E) Southern Outer-Shelf, (F) Southern Inner-Shelf, (G) Off-Shelf, and (H) Marguerite Bay blocks. Block name abbreviations are as in Fig. 1. Median and inter-quartile range (indicated by black error bars in fall and gray shading in winter) of backscattering were calculated in 10-m depth intervals over all observations in each block.

In winter, backscattering decreased by an order of magnitude (i.e. ~10 dB) relative to fall levels within the shallow and middle-depth layers, except in the mid-water layer of Marguerite Bay (Fig. 4B,H and Table 2; Friedman non-parametric two-way analysis of variance test for the effect of season (Sokal and Rohlf, 2000), shallow layer: $\chi^2 = 8$, $p = 0.005$, mid-water layer: $\chi^2 = 4.5$, $p = 0.03$). Significantly different scattering between blocks (Kruskal-Wallis test, $\chi^2 = 510$, $p < 0.001$, $n = 748$) was driven primarily by high scattering in Marguerite Bay and low scattering in

Fig. 4. Interpolated backscattering during fall and winter. Data used for interpolations are the backscattering levels averaged over 1-km along-track intervals. (A,B) Interpolated backscattering 100–300 m. Overlain are contours of bathmetry, showing the 450 and 1000 m isobaths. (C,D) Interpolated backscattering 300–500 m, with bathymetric contours again overlain. (E,F) Interpolated backscattering 100–300 m. Overlain are contours of dynamic height (from Klinck et al., 2004) relative to 400 m. Lows (L) and highs (H) in dynamic topography are indicated, and arrows show the direction of geostrophic flow. (G,H) Interpolated backscattering 25–100 m, with dynamic height contours overlain.

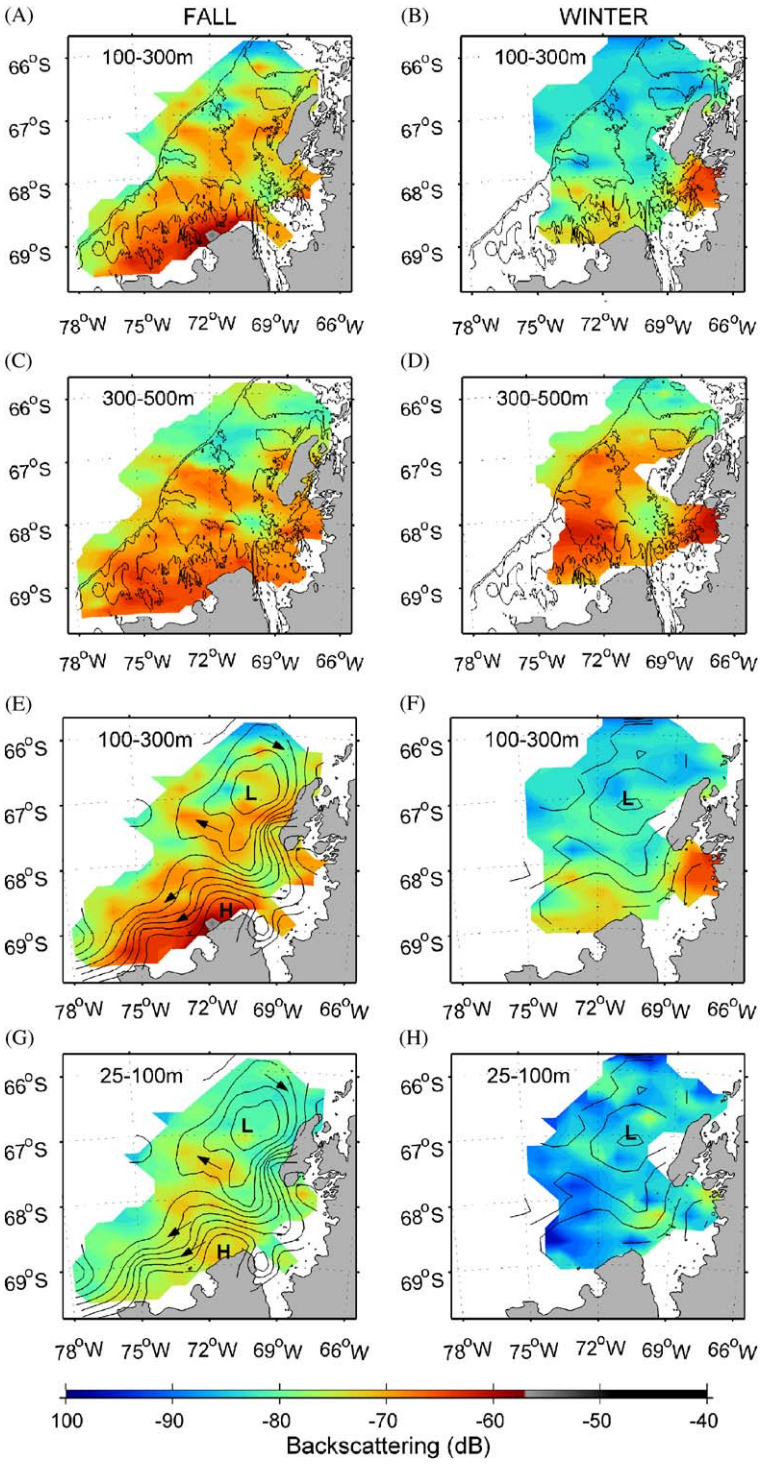
(A)
FALL
100-300m
(B)
WINTER
100-300m
(C)
300-500m
(D)
300-500m
(E)
100-300m
L
H
(F)
100-300m
L
(G)
25-100m
L
H
(H)
25-100m
L
66°S
67°S
68°S
69°S
78°W 75°W 72°W 69°W 66°W
100 -90 -80 -70 -60 -50 -40
Backscattering (dB)

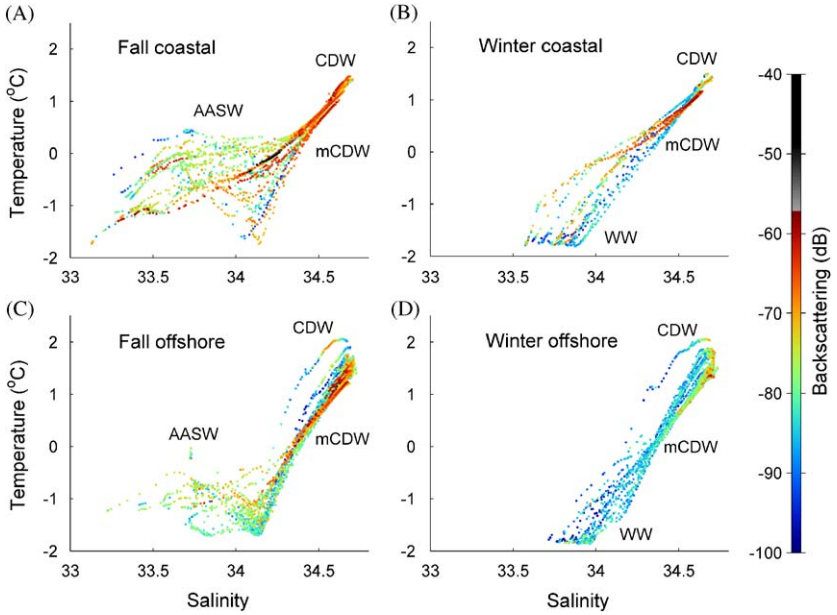

Fig. 5. Potential temperature-salinity diagrams, with dot color indicating backscattering intensity (dB). Data are plotted separately for the (A) fall coastal, (B) winter coastal, (C) fall offshore, and (D) winter offshore blocks. The 'coastal' category includes the three inner-shelf blocks and Marguerite Bay, while the 'offshore' blocks include the outer- and off-shelf blocks. Environmental data were collected at CTD stations (see Klinck et al., 2004). Acoustic backscattering levels represent the acoustic observation (backscattering averaged over 1-km intervals) made nearest to the depth and location of each CTD measurement of temperature and salinity. Note that due to the high sample sizes (9246 in fall, and 6481 in winter), some dots were plotted on top of one another and so low values are somewhat obscured. The water masses present were Antarctic Surface Water (AASW), Circumpolar Deep Water (CDW), modified Circumpolar Deep Water (mCDW), and Winter Water (WW).

the northern and off-shelf blocks (Tukey-Kramer post-hoc tests, $p<0.05$). In the bottom layer (300–500 m; Fig. 4D), backscattering was high over much of the continental shelf, as well as within Marguerite Bay, and did not differ between blocks (Friedman test non-significant; Table 2). Winter backscattering levels showed less of a clear association with the deep troughs across the shelf (Fig. 4B,D). Although there was still evidence from dynamic topography of a weakened gyre in the northern portion of the survey area and a coastal current, there was little evidence of any enhanced backscattering at depth associated with these features (Fig. 4F,H).

3.3.1. Potential impact of vertical migrations on horizontal patterns

In order to determine whether the observed trends in horizontal distribution were confounded by diel vertical migration of the zooplankton responsible for measured backscattering, mean daytime and nighttime backscattering levels in each block were compared within the shallow (25–100 m), mid-water (100–300 m), and deep (300–500 m) layers. Day was defined as 0900–1500, and night as 1700–0700, with dawn and dusk excluded from analysis in order to examine solely whether day or night backscattering differed from one another. If the zooplankton were migrating upwards at night one might expect to see an increase in backscattering in the shallower depth layers from day to night, associated with decreases in the deeper strata. No such pattern consistent with diel vertical migration was observed: comparable backscattering levels were measured in each layer during both day and night in most blocks (Table 2; Mann-Whitney tests $p>0.05$).

3.4. Backscattering relative to water masses

The association between backscattering and particular water masses was explored using observations of potential temperature and salinity from CTD casts (Fig. 5). During fall, highest backscattering levels were associated with modified-CDW. Episodic high values of backscattering also were observed in association with AASW, corresponding to the occasional presence of dense patches in surface waters. Warmer (i.e. less-modified) CDW present in areas farther offshore was typified by generally reduced backscattering, again suggestive of low zooplankton biomass in offshore waters and recent intrusions of CDW on to the continental shelf. In winter, backscattering was lower than in fall, particularly in the more offshore waters and in the WW and colder ($<0.5\,^{\circ}C$) mCDW present at shallower depths (Fig. 5). CDW and warmer mCDW present at depth showed some enhanced scattering, as would be expected from the deep scattering layer observed during the winter survey.

3.5. Multi-variate analyses

Multiple regression analysis with backward step-wise elimination of variables was used to examine how backscattering averaged in 1-km intervals was associated with salinity, fluorescence, transmittance, photosynthetically active radiation (PAR), bottom depth, bottom complexity, distance along-shelf, and distance across-shelf. The standard deviation of the nearest 20 measurements of bottom depth (i.e. within a horizontal distance of ~400 m) was used as a proxy for bottom complexity. Potential temperature, oxygen concentration, and depth were highly correlated with one another and with salinity during both cruises ($r \geqslant 0.8$), and so only salinity was used in the analysis. In fall, distance along-shelf, distance across-shelf, and salinity were the most strongly associated with backscattering levels (standardized partial regression coefficients of −0.53, −0.41, and 0.31, respectively, all p's <0.001). The former two variables had negative effects, indicating that backscattering increased farther in on the shelf and farther along the shelf towards the southwest. Increasing backscattering was associated with increasing salinity, but note that the latter's influence may be due to an association of the zooplankton with salinity itself, or due to the influence of one of its correlates, such as depth. Overall, only 34% of the variation in fall backscattering was accounted for by the selected independent variables ($n = 9246$). In winter, distance along-shelf and salinity were the two most important explanatory variables (standardized partial regression coefficients of −0.50 and 0.46, respectively, p's <0.001), and 41% of the total variation in backscattering was explained by the selected variables ($n = 6481$).

3.6. Taxonomic composition

In general, small (< 2.5 mm in length) and large copepods (>2.5 mm) dominated MOCNESS catches in terms of both numbers and estimated biomass. From qualitative examinations, small copepods were dominated by *Metridia gerlachei* copepodites, with cyclopoids (e.g., *Oithona* and *Oncaea* spp.) also abundant at some locations. The large copepod group was composed of mostly *Calanoides acutus*, *Calanus propinquus*, *Gauidius* spp., adult *M. gerlachei*, *Rhincalanus gigas*, and *Paraeuchaeta* spp. (Ashjian et al., 2004).

Our silhouette method for identifying net catches was not able to identify euphausiids to the level of species. Microscopic examination of a subset of the net catches indicated that the euphausiid community consisted of *E. superba*, *E. crystallorophias*, *E. frigida*, *E. triacantha*, and *Thysanoessa macrura*. For the remainder of this paper, we will group these species together and refer to them simply as euphausiids. Small euphausiids (all individuals <15 mm in length, corresponding to larval stages) often contributed substantially to total zooplankton abundance and biomass, though less than copepods. Large (>15 mm, juveniles and adults) euphausiids made important contributions to sampled biomass, but typically not to abundance. Other taxa, such as pteropods, chaetognaths, amphipods, mysids, siphonophores, other jellies, and micronektonic fishes, were proportionally important only at limited depth ranges and particular locations.

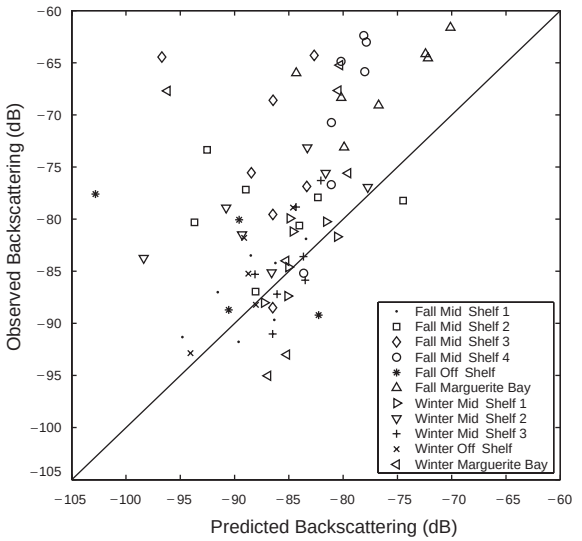

Fig. 6. Comparison of backscattering observed acoustically and that predicted based on the composition of the MOCNESS catches. Observed backscattering levels represent averages over depth ranges equivalent to those sampled by the nets, with individual symbols representing each MOCNESS tow. Acoustic observations were made within 17 km and 5 h of the net tows.

Detailed analyses of MOCNESS catches were performed in a companion study (Ashjian et al., 2004), and the emphasis here is on using these catches to interpret acoustic observations.

Forward calculations of expected backscattering based on net catches showed a positive correlation with observed backscattering levels (Fig. 6; $n = 58$, $r^2 = 0.43$, $p < 1 \times 10^{-7}$). Observed backscattering was generally greater than predicted backscattering, particularly at high levels. The average deviation from a one-to-one relationship was 6.8 dB.These analyses excluded the winter mid-shelf 1 and 2 stations, the two locations where net tows and acoustic data collection were separated in time by approximately a month. Interestingly, however, the predicted backscattering levels for the mid-shelf 1 station fell very close to the 1:1 line. Furthermore, while the predicted backscattering levels for the mid-shelf 2 station were generally lower than observed levels, they were certainly not the most extreme outliers.

The ratios of predicted backscattering for each of the various taxa to total predicted backscattering provide some insight into the possible biological sources of backscattering in the vicinity of each MOCNESS tow. The full set of backscattering predictions for each taxon in each net and tow can be found in Fig. 7; here, only the more noteworthy features will be highlighted.

3.6.1. *Fall sources of backscattering*

Based on fall net catches and taxon-specific acoustic scattering models, large euphausiids were the predicted source of the majority of predicted backscattering at only a few locations and depths: in the mid-water at the mid-shelf 1 and 2 stations (at 22–240 m, and 149–344 m, respectively), at depths where large and diffuse patches were present (Fig. 2A), as well as in the very high scattering and patchy 50–198 m depth range in Marguerite Bay (Fig. 7A). Elsewhere, large euphausiids were either absent or constituted only a minor component of predicted backscattering. Small euphausiids were estimated to make their most important contributions at shallow depths (25–100 m).

Aside from euphausiids, the remainder of the fall predicted backscattering stemmed from a mixture of taxa (Fig. 7A). Large copepods were an important predicted constituent at many stations, particularly below 100 m. Despite never contributing more than 11% of net-sampled biomass (Ashjian et al., 2004), pteropods were occasionally responsible for the majority of predicted backscattering (up to 69%). This is due to the hard shell and associated strong scattering intensity of pteropods in comparison to the more weakly-scattering taxa like euphausiids or copepods (Stanton et al., 1994). Similarly, at certain depths and locations, pneumatophore-bearing siphonophores explained the majority of backscattering. For instance, in the 99–145 m depth stratum at mid-shelf station 3, 66% of backscattering was estimated to result from siphonophores, even though catch biomass in this layer was still dominated by copepods (47%) and the contribution of siphonophores to biomass was negligible (~1%). The pneumatophore structure of siphonophores is a gas-filled sac that scatters a great deal of sound (Warren et al., 2001), evidently overwhelming the contribution to observed backscattering of the biomass-dominating copepods.

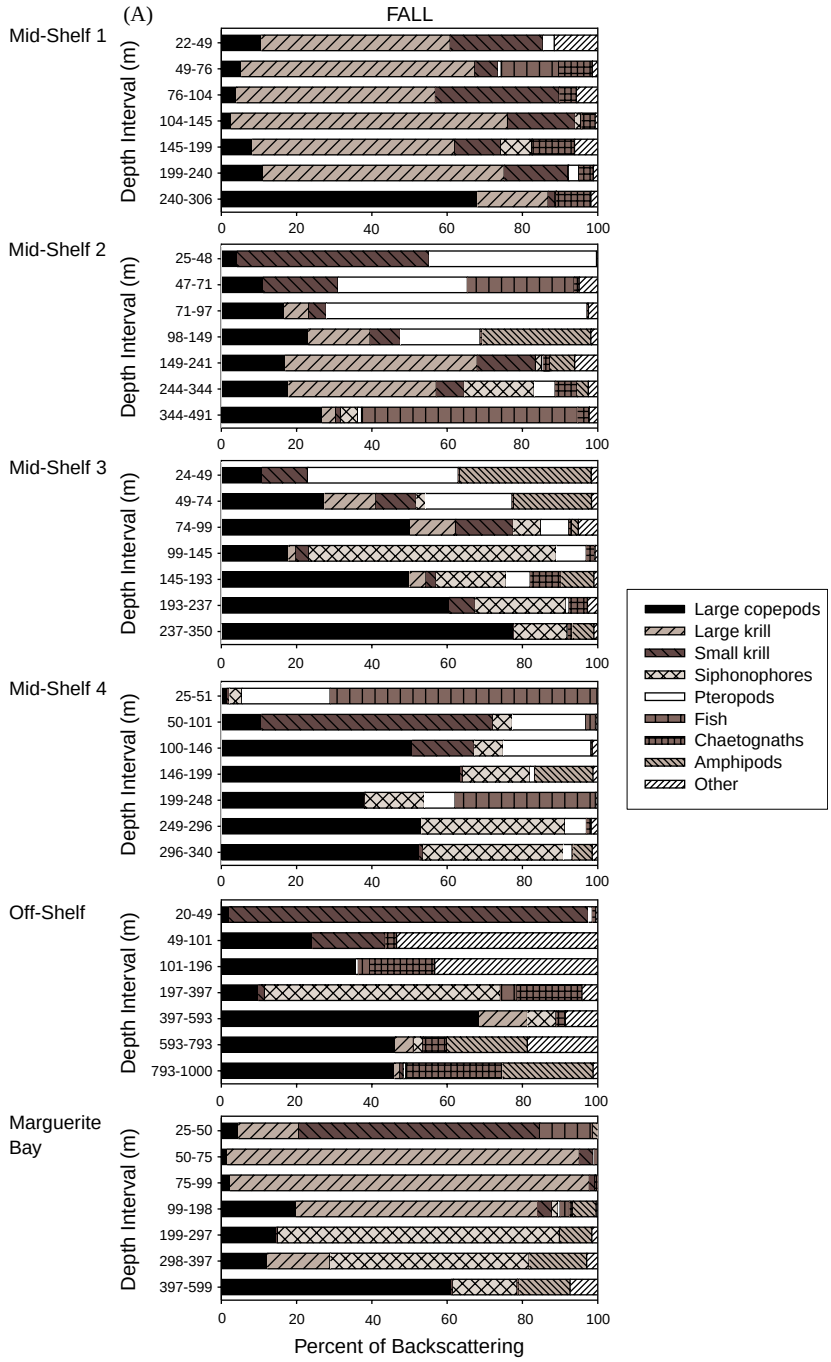

Fig. 7. Predictions of the sources of backscattering based on MOCNESS catches during (A) fall and (B) winter. The percent of total predicted backscattering accounted for by each taxon is shown relative to the depth interval sampled by each net of each tow. The 'pteropod' category refers only to thecosomes (*Limacina* spp.). The 'other' category includes small (<2.5 mm) copepods, medusae, polychaetes, ostracods, eggs, salps, crustacean larvae, radiolarians, mysids, and gymnosome pteropods.

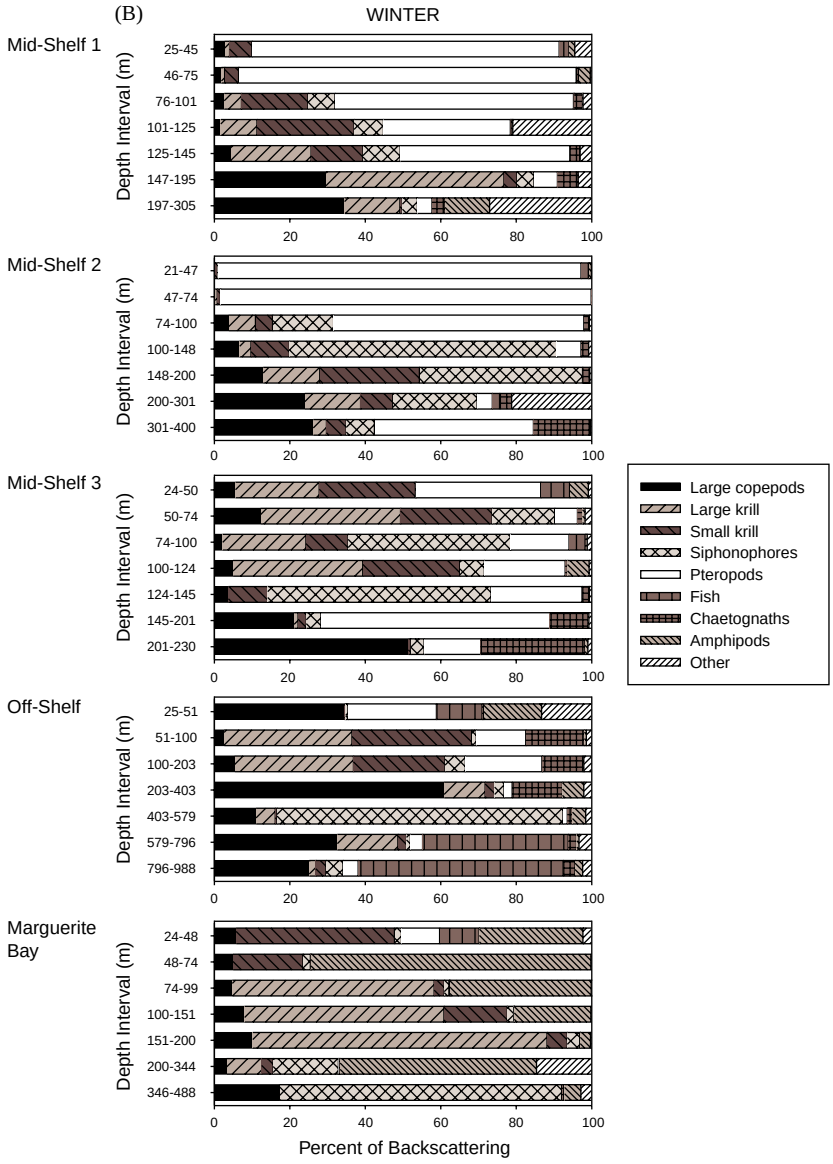

Fig. 7. (*Continued*)

Small copepods frequently dominated catches (up to 72% of biomass), but this taxon never explained more than 19% of predicted backscattering, due to their small size and concomitant weak target strength at 120 kHz.

3.6.2. *Winter sources of backscattering*

In winter, the sources of backscattering predicted from net samples differed from fall (Fig. 7B). The dominant feature observed acoustically in winter was the deep scattering layer found close to the bottom over much of the continental shelf. Unfortunately, difficulties associated with towing the MOCNESS through the pack ice led to problems in sampling this layer. At the mid-shelf 1 station, the deepest net sampled to within 40 m of the bottom. Acoustic data were collected in this region 30 days prior to the net

tow, and at that time, a deep scattering layer was present extending 20–100 m above the bottom. Predictions from the catch composition in this net suggested that large copepods and radiolarians (included in the 'other category' of Fig. 7B) were the dominant contributors to expected backscattering levels in the layer, with smaller contributions from amphipods and large euphausiids. At the mid-shelf 2 station, a scattering layer was present extending 100–150 m off the bottom. Predictions from the deepest net in a tow made 24 days later to within 90 m of the bottom indicated that expected backscattering in the layer was accounted for primarily by pteropods and large copepods. At the mid-shelf 3 station, the deepest net only sampled to within 95 m of the bottom, and therefore passed 25 m above the deep scattering layer observed acoustically. Backscattering in this sampled region immediately above the deep scattering layer was predicted to stem predominantly from copepods and chaetognaths.

Catches from shallower sampled strata suggested that the low backscattering observed outside the deep scattering layer stemmed from a highly complex mixture of taxa (Fig. 7B). Where they were present, siphonophores and pteropods often accounted for most of the predicted backscattering levels. In Marguerite Bay, amphipods were the dominant scatterer in two of the sampled depth intervals, while large euphausiids dominated predicted backscattering in the acoustically intense 151–200 m depth range and in the less intense 74–151 m layer.

4. Discussion

Distinct spatial and seasonal patterns were evident in backscattering levels across the Marguerite Bay continental shelf study area. Clear associations also were observed between backscattering and particular water masses and dynamic topography, which is an indicator of flow. Together with the information derived from net samples on the taxonomic composition of the zooplankton and micronekton responsible for the backscattering, these observations permit important inferences concerning the seasonal distribution, transport, and retention of zooplankton and micronekton biomass in the region.

4.1. Potential limitations of the acoustic technique

The relationship between backscattering at a single frequency and zooplankton biomass is highly complex, and in order to draw any conclusions about biomass on the basis of our acoustic measurements, a number of potentially confounding factors first must be taken into account. Backscattering depends on a number of factors, including the abundance or biomass, taxonomic composition, size, and orientation of scatterers (Stanton and Chu, 2000). In linear echo-integration theory, the echoes from individual animals within the acoustic beam are assumed to sum incoherently, such that echo-integrated backscattering increases with animal abundance. This assumption is valid provided that animal densities are not so high as to cause acoustic attenuation or multiple scattering, and targets can be assumed to be distributed randomly within the beam (MacLennan and Simmonds, 1992); this is likely to be the case here. Inasmuch as biomass increases with abundance, backscattering therefore will also increase with biomass.

Different anatomical classes of zooplankton scatter sound with very different efficiencies, and the taxonomic composition of scatterers has a substantial impact on backscattering. The echo energy scattered per unit biomass of a pteropod, for example, can be 70 times greater than that from a decapod or pneumatophore-bearing siphonophore (Stanton et al., 1994). An observed increase in backscattering therefore could result either from an increase in the biomass of a given taxon of zooplankton, or from a shift in taxonomic composition towards stronger scatterers like pteropods; such a shift even could be accompanied by a decrease in biomass. In the present study, predictions based on net catches of the likely relative contributions of different taxa to observed backscattering levels suggest a highly heterogeneous composition of animals (Fig. 7; note that Section 4.3.1 acknowledges certain limitations of these predictions). There is little evidence that changes in taxonomic composition

might confound our interpretation that the major observed seasonal and spatial differences in backscattering are related to concomitant changes in biomass. The strong-scattering pteropods were predicted to account for more of the backscattering in winter than in fall, suggesting that the decrease in backscattering between the two seasons may be due to an even-larger decrease in biomass than if the taxonomic composition had remained the same. During fall, there was evidence of greater contributions of pneumatophore-bearing siphonophores to backscattering at depths below 100 m in the southern reaches of the survey area and in Marguerite Bay, and an increased importance of euphausiids towards the north. Although backscattering was lower in the north, echo energy per unit biomass is comparable for siphonophores and euphausiids (Stanton et al., 1994), and so this backscattering decrease is more likely related to a difference in biomass than to spatial patterns in community composition.

For the most part, backscattering increases with animal size. Since biomass also increases with size, backscattering should increase with biomass irrespective of whether biomass increases are related to size or abundance. There do exist, however, size ranges for which backscattering and size are negatively related, such that slightly larger (higher biomass) animals have lower backscattering than smaller ones (Stanton and Chu, 2000). For single pings and individual animals, such 'dips' in the scattering vs. size relationship can be quite pronounced, and have the potential to confound the relationship between backscattering and biomass. In this study, however, we integrate backscattering over large depth ranges and horizontal intervals, and thereby average over a very large number of animals. When scattering is averaged over a distribution of animal lengths, the dips in backscattering at particular size ranges are substantially reduced in magnitude, to 5 dB or less (Stanton et al., 1998; Stanton and Chu, 2000). What's more, the sizes of animals encountered in this study mostly avoid the problem of animal size confounding the relationship between backscattering and biomass: the lengths of most of the net-sampled taxa (e.g., copepods, pteropods, siphonophores, and small euphausiids) were much smaller than the length at which the first dip in the backscattering vs. size relationship occurs. Large euphausiids are the only taxon sampled by the nets whose sizes might have been expected to fall within this first dip, but examining the length distributions of this group in net catches suggests that most animals fell on either side of the requisite range of lengths (Ashjian et al., 2004).

Similarly, animal orientation can have a substantial impact on backscattering for individual animals and single realizations, but this effect is much reduced when scattering is averaged over a distribution of aspects. It also seems unlikely that the observed spatial and seasonal patterns in backscattering can be explained simply by variability in the orientation of animals, as this would require complicated spatial and seasonal changes in orientation that are less plausible than differences in biomass.

Animal taxonomic composition, size, and orientation certainly introduce imprecision into the relationship between backscattering and zooplankton and micronekton biomass, and it therefore is not possible to relate backscattering uniquely to biomass. Nonetheless, the present analyses have revealed large spatial and temporal differences in backscattering (greater than 5 dB), which should exceed any imprecision introduced by these confounding factors, allowing us to attribute coarsely these differences to changes in biomass.

There also exists the possibility that some of the observed backscattering stemmed from sources other than zooplankton or micronekton, such as nekton or non-biological sources. It is unlikely that any animals larger than micronekton (e.g., large fishes) contributed substantially to backscattering measurements. Larger animals would be expected to appear in the acoustic record as distinct and recognizable targets, associated with very high backscattering levels. Very few such targets were evident, however, and backscattering levels seldom exceeded −50 dB. Aside from the artifactual backscattering excised from the up-looking transducer's acoustic record described above, we have little information on the possibility of scattering from non-biological sources. Work in the Gulf of Maine has demonstrated that small-scale variations in the temperature and salinity

structure of the water column (i.e. microstructure) may at times scatter sound at levels comparable to backscattering from zooplankton (Warren et al., 2003). Preliminary examinations of acoustic data collected concurrent to casts with a microstructure probe during a later cruise suggest that thin and low-intensity backscattering layers may be associated at times with regions of high microstructure, but such weak scattering is unlikely to contribute substantially to the averages of backscattering under examination in the present study.

Finally, diel vertical migrations by the animals responsible for observed backscattering may introduce uncertainty into our interpretations of distribution. Comparisons of mean backscattering within the different depth strata between day and night do not support this notion, other than perhaps in the shallow layer during winter. Even in this depth range, since the position of the ship in relation to time of day was effectively random, any diel changes in vertical position should simply introduce random error into the acoustic measurements. Diel vertical migration of some component of the zooplankton community undoubtedly does occur (e.g. Zhou and Dorland, 2004 observed distinct diel vertical migrations by individual euphausiid aggregations), but it seems that the influence of such migrations on our large-scale analyses is minor.

4.2. Seasonal changes in backscattering

One of the most striking patterns observed in backscattering levels was the decrease in scattering from fall to winter evident in the upper 300 m of the water column throughout the survey area, other than in Marguerite Bay. In contrast, backscattering below 300 m remained high even in winter, and in fact increased relative to fall levels in Marguerite Bay and the northern and southern outer-shelf. Comparing backscattering levels averaged over the entire sampled depth range (25–500 m) suggests that water-column backscattering in Marguerite Bay and the outer- and off-shelf areas during winter was comparable to or exceeded fall levels (Fig. 8). Over the inner-shelf, winter backscattering was reduced to 6–19% of fall levels. Mean winter backscattering averaged over the entire surveyed area and water column was −69.6 dB, accounting for 32.5% of the backscattering present during fall (mean −64.8 dB). This is indicative of a seasonal decrease in

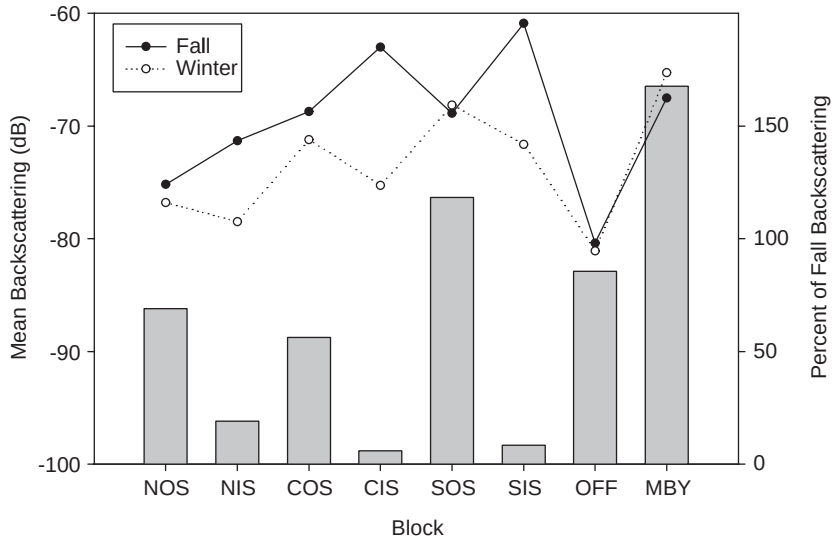

Fig. 8. Mean backscattering levels observed in the entire sampled portion of the water column (25–500 m) in each block, during fall and winter (left *y*-axis). Vertical bars indicate the percent of fall total backscattering in each block that can be accounted for by winter backscattering levels (right *y*-axis). Averages and percentages were calculated using the arithmetic form of backscattering (s_v).

zooplankton biomass, and correspondingly, a decrease in zooplankton biomass between the two seasons also was observed by other instruments. Biomass sampled in the MOCNESS tows described above decreased from fall to winter by approximately 60% (Ashjian et al., 2004). Analyses of optical plankton counter-derived zooplankton size spectra likewise suggested that particle abundance between 0.25 and 14 mm in equivalent spherical diameter decreased between fall and winter of 2002 by 82% (Zhou et al., 2004).

Similar seasonal reductions in the biomass of zooplankton have been observed in studies of other regions of the antarctic continental shelf (e.g. copepods; Schnack-Schiel et al., 1998), and for Antarctic krill in particular (Heywood et al., 1985; Siegel, 1988, 1989; Lascara et al., 1999; and see review in Siegel, 2000). A seasonal decrease in Antarctic krill biomass may not be a consistent feature across all regions, however, as South Georgia typically supports a strong krill fishery during winter (e.g. Murphy et al., 1997). In repeat surveys that overlapped during fall and summer with the northern end of the SO GLOBEC study area, and that in winter and spring covered the continental shelf farther north, Lascara et al. (1999) observed an order of magnitude decrease from spring and summer Antarctic krill biomass levels (32 and 95 $g\,m^{-2}$, respectively) to fall and winter (12 and 8 $g\,m^{-2}$, respectively). In the latter survey, mean biomass was driven primarily by one high-biomass station; biomass was zero at most other stations. These authors calculated biomass by assuming that all backscattering at 120 kHz in excess of −81 dB and above 189 m in depth was Antarctic krill. Although we do not make this scaling from backscattering to biomass, winter backscattering in the present study frequently exceeded −81 dB, and so would have resulted in non-zero biomass estimates by the Lascara et al. (1999) method. However, backscattering levels higher than −81 dB typically were found below 189 m, possibly explaining the many zero winter biomass estimates made in this earlier study.

A number of factors may explain the decrease in zooplankton backscattering from fall to winter. These include vertical and horizontal movements, mortality, and advection of the zooplankton and micronekton in question. It also must be noted in considering these explanations that we are dealing with backscattering as a whole, and that different factors may explain changes in the biomass and distribution of individual taxa.

4.2.1. *Vertical movements*

Downwards seasonal migrations may have contributed to the decrease in overall backscattering levels. Certain taxa, including the large copepods *C. acutus* and *R. gigas*, are known to undergo ontogenetic migrations to deeper waters during winter (Ross et al., 1996). Migration below the depth ranges normally sampled by nets and acoustics has been hypothesized to be a possible cause of apparent seasonal changes in the biomass of Antarctic krill in the present study area (Lascara et al., 1999). Euphausiid biomass at depths below 400 m has typically been found to be low in all seasons (Marin et al., 1991; Ross et al., 1996; Ashjian et al., 2004). There is some evidence, however, that Antarctic krill on occasion may be associated with the bottom, from a bottom-mounted light trap in a shallow water region under fast ice (Kawaguchi et al., 1986), acoustic observations in conjunction with trawl catches (Heywood et al., 1985), and two observations made by a remote-operated vehicle (ROV) within 1 m of the bottom (Gutt and Siegel, 1994).

In the present study, due to the use of a chirp pulse (Ehrenberg and Torkelson, 2000) and to the ability of the BIOMAPER-II to be towed at depths up to 300 m, we were consistently able to sample acoustically to 500 m, occasionally reaching as deep as 550 m. Depending on bathymetry, this allowed us to sample all the way to the bottom over much of the continental shelf. In certain portions of the study area, backscattering in the deepest portions of the water column increased from fall to winter, suggestive of a downwards movement of zooplankton. Overall, however, even including backscattering at the deepest depths surveyed, winter backscattering in the surveyed water column accounted for only 32.5% of observed fall levels. Downwards vertical movements alone therefore may not account for the seasonal decrease in backscattering.

Upwards migration of the zooplankton responsible for backscattering above the minimum sampled range of the acoustic system (25 m) also does not explain the fall to winter decrease. Analyses of MOCNESS catches do not indicate that total zooplankton biomass increased in the 0–25 m depth stratum (Ashjian et al., 2004). Concurrent ROV surveys did observe high abundances of larval euphausiids immediately under the pack ice in many locations during winter, suggesting that larval euphausiids may have migrated to the underside of the ice (Gallager et al., 2002). Since the present analyses indicate that small euphausiids are minor contributors to overall backscattering, such a migration is unlikely to have affected observed backscattering levels.

4.2.2. Horizontal migrations

Horizontal migrations to preferred over-wintering habitats by zooplankton or micronekton may explain some of the winter decrease in backscattering. Adult Antarctic krill are capable of sustained swimming at speeds of 10–15 cm s^{-1} (Kils, 1981), and so in the eight weeks between the fall and winter surveys, could have migrated as far as 725 km. Siegel (1988) hypothesized that adult Antarctic krill migrate offshore in spring, returning to coastal areas for the winter perhaps following a food gradient, and an association of zooplankton with coastal waters during winter has been observed in other shelf regions (Siegel, 1988, 1989; Zhou et al., 1994; Lascara et al., 1999). In the present study, we penetrated through the ice close to shore during winter on only limited occasions. On one of those instances, in Laubeuf Fjord at the northern end of Marguerite Bay, high backscattering was observed, and according to our net-based predictions, much of this backscattering came from large euphausiids. It thus seems possible that large euphausiids may have migrated out of the surveyed area between fall and winter, into the many un-surveyed coastal fjords of Marguerite Bay and its surrounding islands. It appears unlikely, however, that a preference for a particular water mass and a change in the distribution of that water mass would be involved in such a horizontal movement. Temperature-salinity diagrams indicated that backscattering in fall was highest in modified CDW, and similar diagrams from winter data indicate that abundant modified CDW was still present on the shelf.

4.2.3. Mortality

Large zooplanktivorous predators are common in the Marguerite Bay region, and include whales (Thiele et al., 2004), seals (Burns et al., 2004), and birds (Chapman et al., 2004). Such predators may have been responsible for high levels of mortality. Until we gain a detailed understanding of the sources of backscattering and the population dynamics of the various zooplankton taxa, the contribution of mortality to the decrease in backscattering remains unclear.

4.2.4. Transport and retention of zooplankton and micronekton

Advection may have transported zooplankton and micronekton out of the study area, accounting for some of the observed decrease in backscattering between the two seasons. In fall, contours of dynamic height indicated the presence of a large gyre situated over the northern portion of the continental shelf study area; previous studies of the area and analyses of historical datasets suggest that this is a persistent feature of the region (Hofmann et al., 1996; Smith et al., 1999). The southern end of this gyre contained elevated backscattering, suggesting that zooplankton were being transported in an off-shelf direction. Current speeds in the gyre were on the order of 3–15 cm s^{-1} (from ADCP and dynamic height calculations, respectively; Klinck et al., 2004), and in the eight weeks between the two cruises, could have transported the zooplankton between 145 and 725 km in a straight-line direction. Where the southern end of the gyre reached the shelf break and turned towards the north, zooplankton may either have been entrained into the fast-flowing (up to 30 cm s^{-1}, Klinck et al., 2004) Antarctic Circumpolar Current (ACC) and transported to regions farther north, or retained within the gyre structure.

Dynamic height estimates, ADCP measurements, and drifter tracks indicated the presence during fall of a strong coastal current moving towards the southwest along Adelaide and

Alexander Islands (Beardsley et al., 2004; Klinck et al., 2004). High zooplankton backscattering was associated with this physical feature. Although the coastal current passes through areas of complex bathymetry where zooplankton could potentially find refuge, it still likely transported much of the zooplankton found during fall in the southern shelf region towards the southwest and out of the study area. At ADCP-measured speeds of 10–25 $cm\,s^{-1}$ (Klinck et al., 2004), this current could have transported plankton between 480 and 1210 km.

On-shelf flow also may account for some of the seasonal decrease. Hydrographic observations and modeling exercises indicate that warm oceanic CDW is pumped up onto the continental shelf primarily at points where the deep troughs bisecting the shelf meet the shelf break and where the shelf break is strongly curved (Klinck et al., 2004; Dinniman and Klinck, 2004). Maps of interpolated backscattering relative to bathymetry, low levels of backscattering observed in the off-shelf block, analyses of the association between backscattering and water masses, as well as low net-sampled biomass at the off-shelf station (Ashjian et al., 2004), suggest that the oceanic waters being pumped onto the shelf were relatively low in zooplankton. The waters replacing those lost from the study area through other advective features thus may have contributed to the overall decrease in zooplankton and micronekton biomass.

Retentive processes may partially explain why water column backscattering in Marguerite Bay increased from fall to winter: ADCP measurements made by other SO GLOBEC investigators (Zhou et al., 2004; Klinck et al., 2004) suggest the possible existence of a small gyre in the northern end of Marguerite Bay, a notion that is supported by the dynamic height contours presented here. Such a gyre could serve to retain zooplankton in this region, keeping backscattering levels high in both fall and winter.

4.3. Sources of acoustic backscattering

4.3.1. Accuracy of forward calculations

Any inferences about the sources of acoustic backscattering rely on the accuracy of our forward calculations. Forward predictions of backscattering based on net samples were generally lower than observed backscattering levels, particularly at high intensities. A number of factors may have contributed to this discrepancy. First, MOCNESS tows and acoustic samples could not be made at exactly the same times and locations. High spatial and temporal variability in the abundance and composition of zooplankton may have resulted in the two systems sampling different communities. This is particularly true for sparsely or patchily distributed organisms like euphausiids, which may have contributed to the acoustic measurements but been missed by the nets. It is pertinent that in temperate waters typified by generally higher zooplankton densities and where net and acoustic sampling were co-located, forward calculations have yielded more favorable comparisons than seen here (Wiebe et al., 1996; Bucklin et al., 2002). Furthermore, net studies have led to the suggestion that although the absolute biomass of a particular taxon may vary dramatically in space or time, its proportional contribution to total zooplankton biomass is generally much less variable (Wiebe et al., 1992). While spatial and temporal variability thus might contribute to the discrepancy in magnitude between predicted and observed backscattering, the predicted relative contributions of individual taxa may be less subject to such error.

Second, biological characteristics such as length distribution can vary dramatically between even closely spaced Antarctic krill swarms, and a single tow may not provide an unbiased estimate of the length distribution of krill in a given region (Watkins et al., 1986, 1990). Some degree of uncertainty thus will certainly be propagated into our predictions of the sources of backscattering due to error in the net catch data themselves. During the surveys, it generally was not possible to conduct replicate tows in order to quantitatively constrain this error. At the Marguerite Bay station in fall, however, three separate tows were made through a series of dense euphausiids swarms over the course of 18 h and over a spatial area of $16 \times 4.5\,km^2$ (Wiebe et al., 2004). Analysis of the catches indicated a marginally non-significant ($p = 0.065$) difference between tows in euphausiid length.

Third, some of the animals present may have avoided the oncoming net. Larger taxa in particular might have been capable of avoidance, despite our use of a strobe light to reduce such an effect. Larger animals also would produce higher observed backscattering levels, and the greater offset between observed and predicted backscattering at higher scattering levels may support the notion that avoidance partially explains the difference between the two. Similar to the present results, Zhou et al. (1994) found that backscattering levels predicted from net catches of euphausiids became increasingly smaller than levels observed with an ADCP for higher observed values, which they attributed to avoidance on the part of the euphausiids.

Finally, some of the models and parameters used in making forward predictions may not have been appropriate in all instances. For most of the dominant taxa, the models of acoustic scattering used here have been experimentally validated through comparisons of model predictions to measured target strengths of actual individual organisms (Stanton et al., 1998; Table 1). Model parameter values (e.g., animal orientation), however, were occasionally chosen on the basis of very little information (see Table 1). Sensitivity analyses suggest that changing parameter values, while still keeping them within biologically plausible ranges, could increase predicted backscattering by only one to five decibels. Model parameter values alone therefore do not appear to explain fully the difference between predicted and observed backscattering.

4.3.2. *Taxonomic composition of zooplankton and micronekton*

Given the preceding discussion, and since only five or six tows were available per cruise to describe such a large study area, any conclusions concerning the sources of observed backscattering must be approached with caution. Performing the forward calculations furthermore only provides an indication of the relative contribution of each zooplankton and micronekton taxon to total backscattering in a given region, and does not allow the conclusion that these relative contributions have been uniquely determined. Nonetheless, these analyses do allow certain broad inferences.

Backscattering in the study area was found in two general forms: dense patches of elevated backscattering intensity, and more elongated and homogenous layers. In fall, dense and discrete patches were observed primarily in Marguerite Bay, contributing to the high mean backscattering levels and enhanced coefficients of variation in backscattering observed in this region. Forward predictions suggest that these patches were composed of large euphausiids. Large but more diffuse patches also were observed at depth over the northern shelf. The composition of these deep patches is less certain, as we can not be certain that the fall mid-shelf 1 MOCNESS tow actually passed through one of these patches. The catch data do suggest the presence of euphausiids, but myctophid fishes are also known to inhabit these areas. Dense patches were less evident in Marguerite Bay in winter, but the MOCNESS tow suggested that large euphausiids and amphipods made up the majority of the intense scattering layer present below 150 m in this area. Outside of these very distinct patches, the analysis of net samples indicated that the sources of backscattering likely included a complex and variable mixture of taxa.

The dominant backscattering feature in winter was the dense bottom scattering layer. Copepods were predicted to be the dominant scatterer in this layer, although two of the three MOCNESS tows that sampled this layer were the two instances where net tows were separated in time from acoustic data collection by as much as 30 days. It is also possible that some taxa were undersampled to a greater extent by the nets than others, leading to an apparent dominance of these other taxa (e.g., copepods in this instance). This may particularly be the case since predicted backscattering levels were low in comparison to measured levels in the bottom scattering layer, suggesting that some component of the animals scattering sound may have been undersampled. There is, however, little evidence from the current analyses to support the notion that large euphausiids migrated to depth during winter.

4.3.3. Implications to acoustic surveys

An important finding of the present study is that euphausiids accounted for the majority of predicted backscattering only at certain depths and locations within the survey area. Backscattering more typically was predicted to be dominated by copepods, pneumatophore-bearing siphonophores, pteropods, or a complex mixture of taxa. Where they were present, the relatively rare and low-biomass but strongly scattering pteropods and siphonophores appeared to overwhelm the contributions to backscattering of more weakly scattering taxa (similar to observations in the Gulf of Maine and on Georges Bank; Wiebe et al., 1996; Benfield et al., 2003). At 120 kHz, small fluid-like animals like copepods scatter near the transition between the Rayleigh and geometric scattering regions, and so in our predictions from net catches, copepod contributions to overall backscattering never exceeded −80 dB.Although copepod backscattering thus can be filtered out via thresholding if larger animals like euphausiids are of sole interest, such levels are certainly measurable and of consequence in generally low-scattering regions such as the present study site. Furthermore, copepods frequently dominate the zooplankton community in terms of abundance and biomass (Ashjian et al., 2004), and it is noteworthy that acoustic data potentially can provide information on their distribution.

Acoustic surveys in the Antarctic have employed a number of techniques to discriminate euphausiid backscattering from that arising from other scatterers. Often it has been assumed that all measured zooplankton backscattering above some minimum threshold (generally ca. −80 dB) stemmed from Antarctic krill (e.g., Macaulay et al., 1984; Lascara et al., 1999; Nicol et al., 2000). This assumption would lead to over-estimates of Antarctic krill biomass in the present study area, at least. In other instances, visual scrutiny and/or some degree of trawling has been employed to distinguish Antarctic krill patches from other sources of backscattering such as myctophid fishes (Sahrhage, 1989; Sprong and Schalk, 1992; Murray et al., 1995; Pauly et al., 2000), but this approach discards a great deal of potential information on the abundance of taxa other than krill.

Differences in backscattering at two or more discrete frequencies have been used with a great deal of success to identify euphausiid backscattering and filter out returns from other taxa. The range of differences in scattering attributable to particular euphausiid species has been based either on analyses of patches known from net samples to be predominantly mono-specific (Madureira et al., 1993; Brierley et al., 1998; Watkins and Brierley, 2002), in one instance in conjunction with analyses of swarm energetic and shape characteristics (Woodd-Walker et al., 2003), or on theoretical predictions from target strength models (e.g., Hewitt et al., 2003). Such multi-frequency analyses are very promising, and perhaps could be expanded to account for rare, but strongly scattering taxa like pteropods and gas-bearing siphonophores, where they are present.

5. Summary

Distinct spatial and seasonal patterns were evident in zooplankton backscattering across the Marguerite Bay continental shelf study area. During fall, backscattering was highest in the southern reaches of the survey area and inside Marguerite Bay, regions also associated with high abundances of whales, seals, and birds (Thiele et al., 2004; Burns et al., 2004; Chapman et al., 2004, respectively). In winter, the dominant scattering feature was a bottom scattering layer covering much of the continental shelf. Downwards vertical migrations of zooplankton into this bottom layer may have contributed to the observed decrease in backscattering levels from fall to winter in the mid-water, but may not account fully for the decrease in backscattering for the water column as a whole. The latter was probably due to vertical migrations plus a combination of advection out of the survey area, mortality, and horizontal movements. Advection could have occurred either via zooplankton in the northern shelf gyre becoming entrained into the ACC or via the southwest-flowing coastal current. Although the results from the present study concerning the advection of zooplankton are equivocal, the possibility that zooplankton from

the Marguerite Bay region become entrained into the ACC and transported to regions farther north is tantalizing, and would support the hypothesis that Marguerite Bay helps to sustain the large downstream euphausiid populations in the Bransfield Strait and South Georgia regions (Atkinson et al., 2001; Fach et al., 2002). Predictions based on net catches of the sources of observed backscattering levels suggest that euphausiids were the dominant scatterer only at very particular locations and depths. Antarctic acoustic surveys should take care to account for other scatterers, including the abundant, but weakly scattering copepods, and the relatively rare, but strongly scattering pteropods and gas-bearing siphonophores.

Acknowledgments

We gratefully acknowledge the support of all officers and crew of the RVIB *N. B. Palmer* and the staff of Raytheon Polar Services. The tireless efforts of all members of the BIOMAPER-II and MOCNESS teams were greatly appreciated: P. Alatalo, M. Butler, M. Dennett, K. Fisher, A. Girard, J. Peterson, and M. Taylor. We also thank P. Alatalo, N. Copley, P. Hull, and G. Rosenwaks for lab analyses of MOCNESS catches, E. Hofmann, J. Klinck, and all the members of the CTD group for the use of their data and dynamic height estimates, and Sam Johnston of HTI for setting up the acoustic data collection system. D. Chu, A. Lavery, and T. Stanton provided much appreciated assistance with acoustic models, as well as advice concerning the assumptions of the single-frequency technique. Earlier versions of the manuscript benefited substantially from the comments of Jon Watkins and an anonymous reviewer. This project was supported by NSF US Antarctic Program Grant OPP-9910307 to P. Wiebe, C. Ashjian, C. Davis, and S. Gallager. G. Lawson was supported by a Fulbright Scholarship, a Natural Sciences and Engineering Research Council of Canada Post-Graduate Scholarship, and an Office of Naval Research Graduate Traineeship Award in Ocean Acoustics (Grant N00014-03-1-0212). This is GLOBEC contribution number 431 and Woods Hole Oceanographic Institution contribution number 11124.

References

Anderson, V.C., 1950. Sound scattering from a fluid sphere. Journal of the Acoustical Society of America 22, 426–431.

Ashjian, C.J., Rosenwaks, G.A., Wiebe, P.H., Davis, C.S., Gallager, S.M., Copley, N.J., Lawson, G.L., Alatalo, P., 2004. Distribution of zooplankton on the continental shelf off Marguerite Bay, Antarctic Peninsula, during Austral Fall and Winter, 2001. Deep-Sea Research II, this issue [doi:10.1016/j.dsr2.2004.07.025].

Atkinson, A., Whitehouse, M.J., Priddle, J., Cripps, G.C., Ward, P., Brandon, M.A., 2001. South Georgia, Antarctica: a productive, cold water, pelagic ecosystem. Marine Ecology Progress Series 216, 279–308.

Beardsley, R.C., Limeburner, R., Owens, W.B., 2004. Drifter measurements of surface currents near Marguerite Bay on the western Antarctic Peninsula shelf during austral summer and fall, 2001 and 2002. Deep-Sea Research II, this issue [doi:10.1016/j.dsr2.2004.07.031].

Benfield, M.C., Lavery, A., Wiebe, P.H., Greene, C.H., Stanton, T.K., Copley, N.C., 2003. Distributions of physonect siphonulae in the Gulf of Maine and their potential as important sources of acoustic scattering. Canadian Journal of Fisheries and Aquatic Sciences 60, 759–772.

Brierley, A.S., Ward, P., Watkins, J.L., Goss, C., 1998. Acoustic discrimination of Southern Ocean zooplankton. Deep-Sea Research II 45, 1155–1173.

Bucklin, A., Wiebe, P.H., Smolenack, S.B., Copley, N.J., Clarke, M.E., 2002. Integrated biochemical, molecular genetic, and bioacoustical analysis of mesoscale variability of the euphausiid *Nematoscelis difficilis* in the California Current. Deep-Sea Research I 49, 437–462.

Burns, J.M., Costa, D.P., Fedak, M., Bradshaw, C.J.A., Hindell, M.A., McDonald, G., Trumble, S.J., Chittick, E., Gray, M., Gales, N., Barnes, J., Shaffer, S., Kuhn, K., Lovell, P., Crocker, D., 2004. Winter habitat use and foraging behavior of crabeater seals along the Western Antarctic Peninsula. Deep-Sea Research II, this issue [doi:10.1016/j.dsr2.2004.07.021].

Chapman, E.W., Ribic, C.A., Fraser, W.R., 2004. The distribution of seabirds and pinnipeds in Marguerite Bay and their relationship to physical features during austral winter 2001. Deep-Sea Research II, this issue [doi:10.1016/j.dsr2.2004.07.005].

Chu, D., 2000. The GLOBEC Kriging Software Package - EasyKrig2.1, May 1, 2000. WWW Page, http://globec.whoi.edu/software/kriging/easy_krig/easy_krig.html.

Chu, D., Foote, K.G., Stanton, T.K., 1993. Further analysis of target strength measurements of Antarctic krill at 38 and 120 kHz: Comparison with deformed cylinder model and inference of orientation distribution. Journal of the Acoustical Society of America 93, 2985–2988.

Chu, D., Wiebe, P.H., Stanton, T.K., Hammar, T.R., Doherty, K.W., Copley, N.J., Zhang, J., Reeder, D.B., Benfield, M.C., 2000. Measurements of the material properties of live marine organisms and their influence on acoustic scattering. Proceedings of the OCEANS 2000 MTS/IEEE International Symposium, Sept. 11–14, 2000, Providence, RI, Vol. 3, pp. 1963–1967.

Chu, D., Wiebe, P.H., Copley, N.J., Lawson, G.L., Puvanendran, V., 2003. Material properties of North Atlantic cod eggs and early stage larvae and their influence on acoustic scattering. ICES Journal of Marine Science 60, 508–515.

Davis, C.S., Wiebe, P.H., 1985. Macrozooplankton biomass in a warm-core Gulf Stream ring: Time series changes in size structure, taxonomic composition, and vertical distribution. Journal of Geophysical Research 90, 8871–8882.

Davis, C.S., Gallager, S.M., Solow, A.R., 1992. Microaggregations of oceanic plankton observed by towed video microscopy. Science 257, 230–232.

Dinniman, M.S., Klinck, J.M., 2004. A model study of circulation and cross-shelf exchange on the west Antarctic peninsula continental shelf. Deep-Sea Research II, this issue [doi:10.1016/j.dsr2.2004.07.030].

Ehrenberg, J.E., Torkelson, T.C., 2000. FM slide (chirp) signals: a technique for significantly improving the signal-to-noise performance in hydroacoustic assessment systems. Fisheries Research 47, 193–199.

Fach, B.A., Hofmann, E.E., Murphy, E.J., 2002. Modeling studies of antarctic krill *Euphausia superba* survival during transport across the Scotia Sea. Marine Ecology Progress Series 231, 187–203.

Foote, K.G., Stanton, T.K., 2000. Acoustical methods. In: Harris, R.P., Wiebe, P.H., Lenz, J., Skjoldal, H.R., Huntley, M. (Eds.), ICES Zooplankton Methodology Manual. Academic Press, Boston, pp. 223–258.

Foote, K.G., Knudsen, H.P.,Vestnes, G., MacLennan, D.N., Simmonds, E.J., 1987. Calibration of acoustic instruments for fish density estimation: a practical guide. ICES Cooperative Research Report 144.

Gallager, S.M., Daly, K., Fisher, K., Lawson, G., Davis, C.S., Ashjian, C., Wiebe, P.H., 2002. Seasonal changes in the association of larval krill with its potential microplankton food resource along the Western Antarctic Peninsula. Eos, Transactions of the American Geophysical Union, 84, Ocean Sciences Meeting Supplement, Abstract OS51A-13.

Gutt, J., Siegel, V., 1994. Benthopelagic aggregations of krill (*Euphausia superba*) on the deeper shelf of the Weddell Sea (Antarctic). Deep-Sea Research I 41, 169–178.

Hewitt, R.P., Demer, D.A., 2000. The use of acoustic sampling to estimate the dispersion and abundance of euphausiids, with an emphasis on Antarctic krill, *Euphausia superba*. Fisheries Research 47, 215–229.

Hewitt, R.P., Demer, D.A., Emery, J.H., 2003. An 8-year cycle in krill biomass density inferred from acoustic surveys conducted in the vicinity of the South Shetland Islands during the austral summers of 1991–1992 through 2001–2002. Aquatic Living Resources 16, 205–213.

Heywood, R.B., Everson, I., Priddle, J., 1985. The absence of krill from the South Georgia zone, winter 1983. Deep-Sea Research 32, 369–378.

Hofmann, E.E., Klinck, J.M., 1998. Hydrography and circulation of the Antarctic continental shelf: 150°E eastward to the Greenwich Meridian. In: Robinson, A.R., Brink, K.H. (Eds.), The Sea, The Global Coastal Ocean, Regional Studies and Synthesis, Vol. 11, pp. 997–1042.

Hofmann, E.E., Klinck, J.M., Lascara, C.M., Smith, D.A., 1996. Water mass distribution and circulation west of the Antarctic Peninsula and including Bransfield Strait. In: Ross, R.M., Hofmann, E.E., Quetin, L.B. (Eds.), Foundations for ecological Research West of the Antarctic Peninsula, American Geophysical Union, Washington, DC, Antarctic Research Series, Vol. 70, pp. 61–80.

Hofmann, E.E., Klinck, J.M., Costa, D.P., Daly, K.D., Torres, J.J., Fraser, W.R., 2002. US Southern Ocean Global Ocean Ecosystem Dynamics Program. Oceanography 15, 64–74.

Ichii, T., 2000. Krill harvesting. In: Everson, I. (Ed.), Krill: Biology, Ecology and Fisheries. Blackwell Science, Oxford, pp. 228–261.

Kawaguchi, K., Matsuda, O., Ishikawa, S., Naito, Y., 1986. A light trap to collect krill and other micronektonic and planktonic animals under the Antarctic coastal fast ice. Polar Biology 6, 37–42.

Kils, U., 1981. Swimming behavior, swimming performance and energy balance of Antarctic krill *Euphausia superba*. BIOMASS Scientific Series 3, 1–122.

Klinck, J.M., Hofmann, E.E., Beardsley, R.C., Salihoglu, B., Howard, S., 2004. Water-mass properties and circulation on the west Antarctic Peninsula Continental Shelf in Austral Fall and Winter 2001. Deep-Sea Research II, this issue [doi:10.1016/j.dsr2.2004.08.001].

Lascara, C.M., Hofmann, E.E., Ross, R.M., Quetin, L.B., 1999. Seasonal variability in the distribution of Antarctic krill, *Euphausia superba*, west of the Antarctic Peninsula. Deep-Sea Research I 46, 951–984.

Laws, R.M., 1985. The ecology of the Southern Ocean. American Scientist 73, 26–40.

Le Fèvre, J., Legendre, L., Rivkin, R.B., 1998. Fluxes of biogenic carbon in the Southern Ocean: roles of large microphagous zooplankton. Journal of Marine Systems 17, 325–345.

Macaulay, M.C., English, T.S., Mathisen, O.A., 1984. Acoustic characterization of swarms of Antarctic krill (*Euphausia superba*) from Elephant Island and Bransfield Strait. Journal of Crustacean Biology 4 (Spec. No. 1), 16–44.

MacLennan, D.N., Simmonds, E.J., 1992. Fisheries Acoustics. Chapman & Hall, London.

Madureira, L.S.P., Ward, P., Atkinson, A., 1993. Differences in backscattering strength determined at 120 and 38 kHz for three species of Antarctic macroplankton. Marine Ecology Progress Series 93, 17–24.

Marin, V.H., Brinton, E., Huntley, M., 1991. Depth relationships of *Euphausia superba* eggs, larvae and adults near the Antarctic Peninsula, 1986–87. Deep-Sea Research 38, 1241–1249.

Medwin, H., Clay, C.S., 1998. Fundamentals of Acoustical Oceanography. Academic Press, Boston.

Murphy, E.J., Trathan, P.N., Everson, I., Parkes, G., Daunt, F., 1997. Krill fishing in the Scotia Sea in relation to bathymetry, including the detailed distribution around South Georgia. CCAMLR Science 4, 1–17.

Murray, A.W.A., Watkins, J.L., Bone, D.G., 1995. A biological acoustic survey in the marginal ice-edge zone of the Bellingshausen Sea. Deep-Sea Research II 42, 1159–1175.

Nicol, S., Pauly, T., Bindoff, N.L., Wright, S., Thiele, D., Hosie, G.W., Strutton, P.G., Woehler, E., 2000. Ocean circulation off east Antarctica affects ecosystem structure and sea-ice extent. Nature 406, 504–507.

Pauly, T., Nicol, S., Higginbottom, I., Hosie, G., Kichener, J., 2000. Distribution and abundance of Antarctic krill (*Euphausia superba*) off East Antarctica (80–150 E) during the Austral summer of 1995/1996. Deep-Sea Research II 47, 2465–2488.

Priddle, J., Smetacek, V., Bathmann, U., 1992. Antarctic marine primary production, biogeochemical carbon cycles and climatic change. Philosophical Transactions: Biological Sciences 338, 289–297.

Ross, R.M., Quetin, L.B., Lascara, C.M., 1996. Distribution of Antarctic krill and dominant zooplankton west of the Antarctic Peninsula. In: Ross, R.M., Hofmann, E.E., Quetin, L.B. (Eds.), Foundations for Ecological Research west of the Antarctic Peninsula, American Geophysical Union, Washington DC, Antarctic Research Series, vol. 70, pp. 199–218.

Sahrhage, D., 1989. Hydroacoustic detection of krill during "Polarstern" cruises ANT V/1 and ANT VI/2 (1987). Archiv für Fischereiwissenschaft 39, 73–80.

Sameoto, D., Cochrane, N., Herman, A.W., 1993. Convergence of acoustic, optical, and net-catch estimates of euphausiid abundance: use of artificial light to reduce net avoidance. Canadian Journal of Fisheries and Aquatic Science 50, 334–346.

Schnack-Schiel, S.B., Hagen, W., Mizdalski, E., 1998. Seasonal carbon distribution of copepods in the eastern Weddell Sea, Antarctica. Journal of Marine Systems 17, 305–311.

Siegel, V., 1988. A concept of seasonal variation of krill (*Euphausia superba*) distribution and abundance west of the Antarctic Peninsula. In: Sarhage, D. (Ed.), Antarctic Ocean and Resources Variability. Springer, Berlin, Heidelberg, pp. 219–230.

Siegel, V., 1989. Winter and spring distribution and status of the krill stock in Antarctic Peninsula waters. Archiv für Fischereiwissenschaft 39, 45–72.

Siegel, V., 2000. Krill (Euphausiacea) demography and variability in abundance and distribution. Canadian Journal of Fisheries and Aquatic Sciences 57 (Suppl. 3), 151–167.

Smith, D.A., Hofmann, E.E., Klink, J.M., Lascara, C.M., 1999. Hydrography and circulation of the west Antarctic Peninsula continental shelf. Deep-Sea Research I 46, 925–949.

Sokal, R.R., Rohlf, F.J., 2000. Biometry: The Principles and Practice of Statistics in Biological Research. W.H. Freeman and Co., New York.

Sprong, I., Schalk, P.H., 1992. Acoustic observations on krill spring-summer migration and patchiness in the northern Weddell Sea. Polar Biology 12, 261–268.

Stanton, T.K., Chu, D., 2000. Review and recommendations for the modelling of acoustic scattering by fluid-like elongated zooplankton: euphausiids and copepods. ICES Journal of Marine Science 57, 793–807.

Stanton, T.K., Wiebe, P.H., Chu, D., Benfield, M.C., Scanlon, L., Martin, L., Eastwood, R.L., 1994. On acoustic estimates of zooplankton biomass. ICES Journal of Marine Science 51, 505–512.

Stanton, T.K., Chu, D., Wiebe, P.H., 1998. Sound scattering by several zooplankton groups. II. Scattering models. Journal of the Acoustical Society of America 103, 236–253.

Thiele, D., Chester, E., Moore, S., Širovic, A., Hildebrand, J., Friedlaender, A., 2004. Seasonal variability in whale encounters in the Western Antarctic Peninsula. Deep-Sea Research II, this issue [doi:10.1016/j.dsr2.2004.07.007].

US Southern Ocean GLOBEC, 2002. Report of the RVIB Nathaniel B. Palmer Cruise 02-02 to the Western Antarctic Peninsula, 9 April to 21 May 2002. United States Southern Ocean Global Ocean Ecosystems Dynamics Program Report Number 9. Old Dominion University, Norfolk, VA. 190pp.

Voronina, N.M., 1998. Comparative abundance and distribution of major filter-feeders in the Antarctic pelagic zone. Journal of Marine Systems 17, 375–390.

Warren, J.D., Stanton, T.K., Benfield, M.C., Wiebe, P.H., Chu, D., Sutor, M., 2001. In situ measurements of acoustic target strengths of gas-bearing siphonophores. ICES Journal of Marine Science 58, 740–749.

Warren, J.D., Stanton, T.K., Wiebe, P.H., Seim, H.E., 2003. Inference of biological and physical parameters in an internal wave using multiple-frequency, acoustic-scattering data. ICES Journal of Marine Science 60, 1033–1046.

Watkins, J.L., Brierley, A.S., 2002. Verification of the acoustic techniques used to identify Antarctic krill. ICES Journal of Marine Science 59, 1326–1336.

Watkins, J.L., Morris, D.J., Ricketts, C., Priddle, J., 1986. Differences between swarms of Antarctic krill and some implications for sampling krill populations. Marine Biology 93, 137–146.

Watkins, J.L., Morris, D.J., Ricketts, C., Murray, A.W.A., 1990. Sampling biological characteristics of krill: effect of heterogeneous nature of swarms. Marine Biology 107, 409–415.

Weeks, A.R., Griffiths, G., Roe, H., Moore, G., Robinson, I.S., Atkinson, A., Shreeves, R., 1995. The distribution of acoustic backscatter from zooplankton compared with physical structure, phytoplankton and radiance during the spring bloom in the Bellingshausen Sea. Deep-Sea Research II 42, 997–1019.

Wiebe, P.H., Morton, A.W., Bradley, A.M., Backus, R.H., Craddock, J.E., Cowles, T.J., Barber, V.A., Flierl, G.R., 1985. New developments in the MOCNESS, an apparatus for sampling zooplankton and micronekton. Marine Biology 87, 313–323.

Wiebe, P.H., Copley, N.J., Boyd, S.H., 1992. Coarse-scale horizontal patchiness and vertical migration of zooplankton in Gulf Stream warm-core ring 82-H. Deep-Sea Research 39 (Suppl. 1), S247–S278.

Wiebe, P.H., Mountain, D., Stanton, T.K., Greene, C., Lough, G., Kaartvedt, S., Manning, J., Dawson, J., Martin, L., Copley, N., 1996. Acoustical study of the spatial distribution of plankton on Georges Bank and the relation of volume backscattering strength to the taxonomic composition of the plankton. Deep-Sea Research II 43, 1971–2001.

Wiebe, P.H., Stanton, T.K., Greene, C.H., Benfield, M.C., Sosik, H.M., Austin, T., Warren, J.A., Hammar, T., 2002. BIOMAPER II: An integrated instrument platform for coupled biological and physical measurements in coastal and oceanic regimes. IEEE Journal of Oceanic Engineering 27, 700–716.

Wiebe, P.H., Ashjian, C., Gallager, S., Davis, C., Lawson, G.L., Copley, N., 2004. Using a high powered strobe light to increase the catch of Antarctic krill. Marine Biology 144, 493–502.

Woodd-Walker, R.S., Watkins, J.L., Brierley, A.S., 2003. Identification of Southern Ocean acoustic targets using aggregation backscatter and shape characteristics. ICES Journal of Marine Science 60, 641–649.

Zhou, M., Dorland, R.D., 2004. Aggregation and vertical migration behavior of *Euphausia superba*. Deep-Sea Research II, this issue [doi:10.1016/j.dsr2.2004.07.009].

Zhou, M., Nordhausen, W., Huntley, M., 1994. ADCP measurements of the distribution and abundance of euphausiids near the Antarctic Peninsula in winter. Deep-Sea Research I 41, 1425–1445.

Zhou, M., Zhu, Y., Peterson, J.O., 2004. In situ growth and mortality of mesozooplankton during the austral fall and winter in Marguerite Bay and its vicinity. Deep-Sea Research II, this issue [doi:10.1016/j.dsr2.2004.07.008].